REGULATION OF CALCIUM SIGNALING BY p130PH IN ASTROCYTES

A Thesis presented to
the Faculty of the Graduate School
at the University of Missouri

In Partial Fulfillment of the Requirements for the Degree

Master of Science

---

by
WENJU CUI

Dr. Shinghua Ding, Thesis Supervisor

MAY 2009

The undersigned, appointed by the dean of the Graduate School, have examined the thesis entitled

REGULATION OF CALCIUM SIGNALING BY p130PH IN ASTROCYTES

presented by Wenju Cui,

a candidate for the degree of Master of Science,

and hereby certify that, in their opinion, it is worthy of acceptance.

Shinghua Ding, Ph.D., Department of Biological Engineering

Kevin D. Gillis, D.Sc., Department of Biological Engineering

Edward H. Blaine, Ph.D., Department of Medical Pharmacology and Physiology

ACKNOWLEDGEMENTS

I came, I saw, I conquered.
----Julius Caesar.

According to Plutarch, these are the words by which Julius Caesar succinctly described one of his victories. And this is so true with me while attaining my MS degree. However, without being so aggressive, I'd rather describe this tiny moment in my life as: I came, I saw, I learned.

July 31st 2007, I flew across the Pacific Ocean, from a city called Dalian, where I've lived for 23 years, to a small town called Columbia in the US. I do not want to touch any detail about living in a totally different country, and it's not merely about getting a MS degree. However, after going through all those crying and laughing moments, I am proud to say I've grown up and am tough enough to face my life.

I really have tons of people to thank. Without them, I wouldn't be able to make it this far. This thesis could not have been well accomplished without my supervisor Dr. Shinghua Ding's help. I thank him very much for making the lab such a pleasant place to work.

I thank Dr. Tiannan Wang, Dr. Min Li, Cindy Chu and Dr. Hwang's lab as a whole for their patience and kindness in guiding me through the thesis process.

I thank Dr. Kevin D. Gillis for serving as my committee member and helping with revising my thesis. Also, many thanks to Ms. JoAnn Lewis for all her help and efforts in supporting our graduate students.

I thank the department of Biological Engineering, Dalton Cardiovascular Research Center and University of Missouri for providing me the opportunity to pursue my higher education. I also thank the entire faculty and staff members for their support.

I thank all my dear friends both in China and here for their warm help and encouragement.

Most importantly, I would like to sincerely thank Dr. Edward H. Blaine who not only served as my committee member but also a wonderful mentor for my life. He's always on my side and giving out valuable suggestions and advices.

In the end, I would like to dedicate this work to my beloved parents, who always love me, support me, cherish me, encourage me and have faith in me no matter where I am and who I am. In their eyes, I am the best daughter in the whole world. They make me want to be better. I would do everything to let them know how much I love them and how grateful I am to be their daughter.

English is not my native language and always, I am wordless when I am truly touched. This little page can tell only this much about my feelings, however, my heart is full of appreciation and I always know how lucky I am to have you all.

Back to the beginning, I came, I saw, I learned, and I'm so much looking forward to the day that I can step on my motherland again.

April 22, 2009

TABLE OF CONTENTS

LIST OF FIGURES

Figure Page

LIST OF TABLES

REGULATION OF CALCIUM SIGNALING BY p130PH IN ASTROCYTES

Wenju Cui

Dr. Shinghua Ding, Thesis Supervisor

ABSTRACT

Ca^{2+} signaling is a characteristic form of astrocyte excitability and has been suggested to mediate chemical transmitter release, including glutamate, but its role in ischemia is not clearly understood. Our previous study (Ding et al., 2009) demonstrated that astrocytes exhibit enhanced Ca^{2+} signaling following photothrombosis-induced ischemia. Given that astrocytes intimately contact neurons to form tripartite synapses and can release glutamate in response to Ca^{2+} elevation, we hypothesize that astrocytes contribute to brain damage through glutamate release. The goal of this thesis is to test this hypothesis by selectively inhibiting astrocytic Ca^{2+} signaling *in vivo* using a Ca^{2+} chelator BAPTA-AM and a molecular approach. Our study has demonstrated that BAPTA-AM significantly reduces ischemia-induced brain damage, suggesting a protective role of BAPTA in ischemia. For more mechanistic studies, we introduced an inositol 1, 4, 5-trisphosphate (IP_3) binding protein p130PH into astrocytes to selectively disrupt IP_3-dependent Ca^{2+} signaling pathway in astrocytes. Results from an *in vitro* study demonstrated that expression of p130PH in cultured astrocytes significantly reduced ATP stimulated Ca^{2+} signals. In order to introduce p130PH *in vivo*, we have developed recombinant adeno-associated virus (rAAV) vectors, which encode astrocyte-specific promoter ABC1D and p130PH. Viral vectors were injected into the cerebral cortexes of mice to test the gene expression pattern. Immunohistochemistry staining including GFAP,

NeuN and Iba1 staining has shown that p130PH was specifically expressed in astrocytes, not in neuron or microglia. Further study will be focusing on determining whether p130PH will have a protective effect on brain damage and neuronal death after photothrombosis induced cerebral ischemia.

Our work will provide novel evidence that astrocytes contribute to brain injury after ischemia, and the inhibition of astrocytic Ca^{2+} mobilization might be a promising target for stroke therapy. The current study will also provide an *in vivo* approach for the treatment of glia-related diseases as well as for the study on neuron-glia interactions in general.

Key words: Astrocytes; IP_3; Ca^{2+} signaling; p130PH; Glutamate release; Neurotransmitter; Stroke

CHAPTER 1

INTRODUCTION

1.1. Neurons in the central nervous system (CNS)

The central nervous system (CNS) is the part of the nervous system that functions to coordinate the activity of all parts of the bodies of multicellular organisms. In vertebrates, the central nervous system is enclosed in the meninges. It contains the majority of the nervous system and consists of the brain, and the spinal cord. It has a fundamental role in the control of behavior. The CNS is contained within the dorsal cavity, with the brain in the cranial cavity, and the spinal cord in the spinal cavity (Maton et al., 1993). The nervous system contains two classes of cell, the neuron and glia (Figure 1.1).

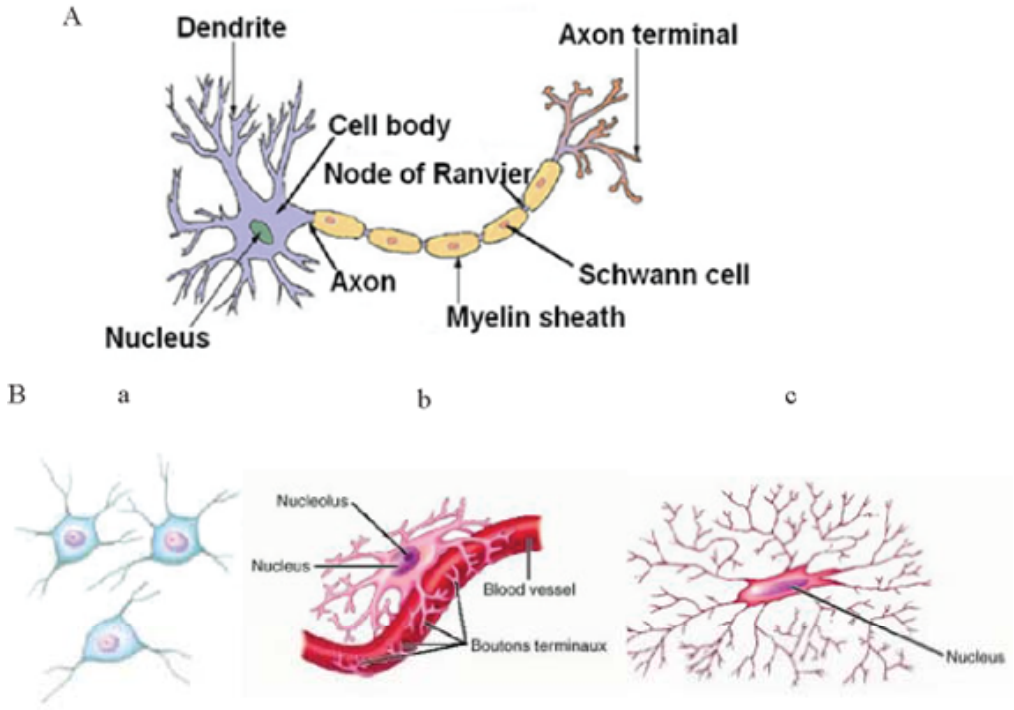

Figure 1.1. Cell types in CNS. (A) Structure of a typical neuron (SEER's Training Website, access date: Apr. 22, 2009). (B) Glia: a. Oligodendrocyte; b. Astrocyte; c. Microglia (medical-dictionary, access date: Apr. 22, 2009)

A neuron (Figure 1.1 A) has a cell body with a nucleus surrounded by cytoplasm containing various organelles, just like other cells. Long processes extend from the cell body and the number and length of the processes can vary. There are usually several dendrites, and the dendrites normally branch and form dendritic "trees" with a large surface to receive signals from other nerve cells. However, there is only one axon for each neuron, which is specially built to conduct the nerve impulse from the cell body to other cells.

Communication between nerve cells takes place at synapses. The synapse is where information is transmitted from one neuron to another. This transmission occurs by liberation of signal molecules which will subsequently influence the other neurons (not by direct propagation of the nerve impulse from one neuron to another). This signal molecule is called a neurotransmitter or a transmitter for short. The neurotransmitter is located in small vesicles called synaptic vesicles. Once a neuron is stimulated by actions from another neuron, the signal is conveyed to the next neuron by the presynaptic release of neurotransmitters. Then, the nerve impulse, which is a traveling membrane voltage signal, is transformed to a chemical signal. The neurotransmitter binds briefly to receptor molecules in the postsynaptic membrane, which has many ion channels, and these channels might associate with the receptor and their opening state may be changed when the transmitter binds to the receptor.

Transmitter release is Ca^{2+}-dependent. The normal event preceding transmitter release is the depolarization of the presynaptic membrane. The release of the transmitter depends on Ca^{2+} entering the bouton (the club-shaped enlargements at the terminal branches of an axon) through voltage-gated calcium channels which are opened by

depolarization. Ca^{2+} flux through channels causes more release of the transmitter (Brodal, 1998).

1.2. Glial cells in CNS

Besides neurons, there is another type of cell in the CNS, generally called a glial cell. Although much research has been done on neurons since they were considered to be essential for nervous system function, recent studies have shown the diversity of roles played by glial cells in nervous system function, thus glial cells are emerging from the background to become more prominent. Furthermore, the significant discovery that the application of the chemical transmitter glutamate induces Ca^{2+} oscillations and Ca^{2+} waves between cultured hippocampal astrocytes (Charles et al., 1991) has sparked the imagination of neuroscientists. Nevertheless, only by modern methods has it been possible to directly study the properties and functional roles of glia, and much still remains unknown. In modern scientific research, the study of glial cells has been greatly facilitated by immunocytochemical methods which identify certain cytoplasmic or surface molecules.

All glial cells (Figure 1.1 B) are equipped with processes and outnumber neurons; however, they are not responsible for the conduction of impulses. The name results from the belief that the glial cells mainly serve as “glue”, keeping the neurons together. There are three main kinds of glial cells: astrocytes (astroglia, Figure 1.1 B b), oligodendrocytes (oligodendroglia, Figure 1.1 B a), and microglial cells (microglia, Figure 1.1 B c). Each is different from the others structurally and functionally (Brodal, 1998).

In this research, we focused specifically on astrocytes to study their Ca^{2+} signaling and other related properties, especially the mechanisms of Ca^{2+}-dependent glutamate release from astrocytes and its effects on the brain damage caused by ischemia.

1.2.1. Astrocytes

Astrocytes are a sub-type of the glial cells in the brain and spinal cord, which are also known as astrocytic glial cells. They are characteristic star-shaped glial cells and their many processes envelope synapses made by neurons. Astrocytes are classically identified histologically by the intermediate filament glial fibrillary acidic protein (GFAP) which is expressed specifically in astrocytes.

Astrocytes have either short or long processes and may be divided into two categories on this basis: protoplasmic astrocytes and fibrillary astrocytes. The processes extend in all directions, and most of the capillary surface is covered by astrocytic processes, and astrocytes play an important role for the capillary permeability to certain substances. Astrocytes also intimately contact neurons and this enables them to exchange substances. In addition, astrocytes form a continuous, thin sheet at the boundary between nervous tissue and connective tissue. Such a limiting membrane can be found around the large vessels and on the inside of the coverings of the brain and spinal cord (Brodal, 1998).

Astrocytes perform many functions, such as biochemical support of endothelial cells which form the blood-brain barrier; the provision of nutrients to the nervous tissue, since it is believed that astrocytes can take up nutrients and metabolites from the blood and then distribute them to other brain cells, such as neurons; a principal role in the repair and

scarring process of the brain and spinal cord following traumatic injuries and the contribution to the regulation of the blood flow during neuronal activity.

1.2.2. Oligodendrocytes and microglia

In addition to astrocytes, there are another two types of glial cells: oligodendrocytes and microglia.

An oligodendrocyte has rather few and short processes, and its cell body is often closely apposed to a neuronal perikaryon, hence oligodendrocytes are also called satellite cells. Oligodendrocytes function to facilitate myelination of axons in the CNS; however, their position in relation to nerve cell somata indicates that they also have other functions, which are still under study.

Microglia, as the third kind of glial cell, is called microglia because of their small size. Microglia may constitute 5%-20% of all glial cells, and are evenly distributed throughout the CNS. There is an assumption, which has been argued for a long time, saying that microglial cells were initially considered to be of mesodermal origin. They had probably invaded the nervous system during embryonic development. Recent immunocytochemical studies agree with this. After invading the nervous tissue, the cells undergo morphological changes which become microglial cells as they are in the adult (Brodal, 1998).

1.3. Astrocytic calcium signaling: inositol 1, 4, 5-trisphosphate (IP_3) messenger pathway

Astrocytes are now widely regarded as cells that propagate intercellular Ca^{2+} waves over long distances in response to stimulation, and similar to neurons, release transmitters (called gliotransmitters) in a Ca^{2+}-dependent manner. The study of the astrocytes' role in signaling transduction is a rapidly growing field of neuroscience (Fiacco et al., 2009).

Chemical transmitters evoke elevated Ca^{2+} in cultured astrocytes (Cornell-Bell et al., 1990). The elevations are predominantly mediated by Gq-linked G-protein coupled receptors (GPCRs) signaling pathway (Fiacco et al., 2009). As an excitable system, in astrocytes, the glutamate-induced Ca^{2+} oscillations are caused by the activation of class I metabotropic glutamate receptors following which inositol trisphosphate (IP_3) is released upon activation of a phospholipase. IP_3 can stimulate the release of Ca^{2+} from IP_3-sensitive internal stores. It is these Ca^{2+} waves, which propagate between cultured astrocytes that direct researchers' attention to identify the mechanism of signal propagation. We all believe that understanding the mechanism of Ca^{2+} wave propagation will provide significant insight into signals that can be released from astrocytes.

There are two prominent hypotheses about Ca^{2+} wave that guide this study: 1) IP_3 could diffuse through gap junctions to evoke Ca^{2+} signals in neighboring unstimulated astrocytes. 2) a message, i.e., ATP, is released from an astrocyte which, by activating P2Y receptors on adjacent astrocytes, stimulates additional Ca^{2+} signals (Haydon and Carmignoto, 2006). It is also possible that both pathways contribute to wave propagation, and a lot of studies have shown that Ca^{2+} oscillations are restricted to portions of the

processes of individual cells, the so-called microdomains. Large distances are not necessary; Ca^{2+} wave can propagate even within one astrocyte. Study has also proved that activation of a single cell can evoke Ca^{2+} increase in neighboring astrocytes, although the range of this signal can be very small compared with those observed in cultured astrocytes (Sul et al., 2004).

Ca^{2+} elevations in astrocytes are predominantly mediated by Gq-linked G-protein coupled receptors (GPCRs) signaling pathway. Stimulation of GPCRs activates phospholipase C (PLC) to liberate the second messenger inositol 1, 4, 5-trisphosphate (IP_3). Elevation of IP_3 then causes the intracellular Ca^{2+} increase through the activation of IP_3 receptors (Haydon, 2001).

Inositol 1, 4, 5-trisphosphate (IP_3): Inositol trisphosphate or inositol 1, 4, 5 - trisphosphate (also commonly known as triphosphoinositol; abbreviated $InsP_3$ or IP_3, Figure 1.2), is a second messenger molecule used in signal transduction in cells. It is made by hydrolysis of phosphatidylinositol 4, 5-bisphosphate (PIP_2), a phospholipid which is located in the plasma membrane, by phospholipase C (PLC).

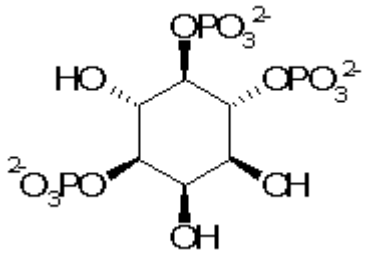

Figure 1.2. Structure of inositol 1, 4, 5-trisphosphate (wikipedia, access date: Apr. 22, 2009).

IP_3 binds to and activates the $InsP_3$ receptor on the membrane of the endoplasmic

reticulum (ER), resulting in the release of Ca^{2+} into the cytoplasm and elevation of cytoplasmic Ca^{2+} levels (Figure 1.3) (Ferris and Snyder, 1992).

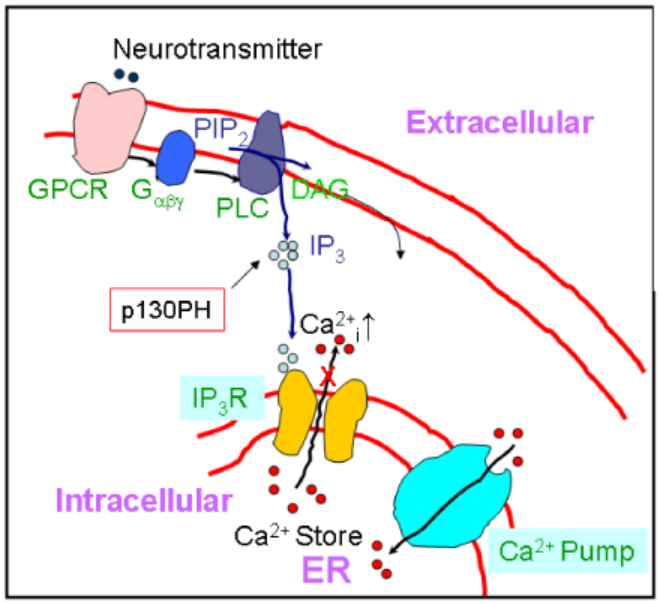

Figure 1.3. Illustration of GPCR-PLC signaling pathway and IP_3-mediated Ca^{2+} release from internal store. p130PH is expected to effectively reduce IP_3 concentration by binding with IP_3, thus reducing Ca^{2+} release from internal store.

It is already clear that inositol 1, 4, 5-trisphosphate (IP_3) -induced Ca^{2+} liberation from internal stores results in the elevation of Ca^{2+}, and this Ca^{2+} signal can control a wide spectrum of cell functions, including energy metabolism, gene transcription, and cell proliferation (Lin et al., 2005).

Inositol triphosphate receptor (IP_3R): Inositol triphosphate receptor (IP_3R) is a membrane glycoprotein complex, and also a Ca^{2+} permeable ion channel activated by inositol triphosphate (IP_3). The IP_3 receptor was first purified from rat cerebellum (Foskett et al., 2007). The IP_3R complex is formed of four 313 kDa subunits. Type 2 IP_3R

(IP_3R2) is the predominant isoform in astrocytes (Fiacco et al., 2009). The IP_3Rs are mainly found in the cell integrated into the endoplasmic reticulum (ER).

Inhibition of Ca^{2+} elevation by p130PH: According to the GPCR-PLC signaling pathway and IP_3-mediated Ca^{2+} release from astrocytes, there are many possible ways to inhibit the Ca^{2+} elevation in astrocytes. One way is to inhibit the GPCR. However, there are many similar kinds of GPCR in neurons and astrocytes in brain tissues, thus inhibition specificity is limited. The strategy to inhibit the IP_3 pathway seems more promising. Within this pathway, there are only two targets we could possibly work on, one is the IP_3 molecule, and the other is IP_3R. A previous study done by Dr. György Hajnóczky's group (Lin et al., 2005) indicated the possibility to inhibit the IP_3 pathway by using certain IP_3 binding proteins. They evaluated the role of IP_3 in the local control mechanisms that support the propagation of Ca^{2+} waves, store operated Ca^{2+} entry, and mitochondrial Ca^{2+} uptake. They tried two types of IP_3-binding proteins (IP_3BP) in their work: 1) the PH domain of the phospholipase C-like protein, p130 (p130PH); and 2) the ligand-binding domain ($IP_3R_{224–605}$) of the human type-I IP_3R. Since we are utilizing p130PH in our study, we will only refer to this protein.

Protein p130 was isolated from rat brain as an IP_3BP. It lacks catalytic activity and has been shown to be important in the signaling by $GABA_A$ receptors (Lin et al., 2005). The module which actually interacts with IP_3 is its pleckstrin homology domain (PH domain). The PH domain is a protein domain of approximately 120 amino acids that occurs in a wide range of proteins involved in intracellular signaling or as constituents of the cytoskeleton (Baltimore et al., 1993). This domain can bind phosphatidylinositol

lipids within biological membranes (such as phosphatidylinositol 3, 4, 5-trisphosphate and/or PIP_2), and proteins such as the βγ-subunits of heterotrimeric G proteins and protein kinase C. Through these interactions, PH domains play a role in recruiting proteins to different membranes, thus targeting them to appropriate cellular compartment or enabling them to interact with other components of the signal transduction pathways (Hemmings et al., 1993). However, for several PH domains, it is not clear whether membrane localization via lipid binding or binding to soluble inositol phosphates is more important for their regulation (Várnai et al., 2002).

Among several PH domains, the only conserved residue is a single tryptophan located within the alpha helix that serves to nucleate the core of the domain. The common 3D structure (Riddihough, 1994) usually contains two perpendicular anti-parallel beta sheets, followed by a C-terminal amphipathic helix. The loops connecting the beta-strands differ greatly in length, making the PH domain relatively difficult to detect while providing the source of the domain's specificity.

According to all the information and research results we gathered from previous studies, we finally chose p130PH as our IP_3 pathway inhibitor. Protein p130PH can interact with IP_3 molecules released from the activation of GPCR-PLC signaling pathway, thus the number of free IP_3 molecules inside the cell is decreased. The probability for the interaction between IP_3 and IP_3R is greatly lowered, which results in the decrease of Ca^{2+} elevation in astrocytes and eventually will cause the reduction of Ca^{2+}-dependant glutamate release from astrocytes.

1.4. Glutamate release from astrocytes and neuron-glia interactions

1.4.1. Mechanisms of glutamate release from astrocytes

There are several mechanisms of glutamate release, and studies have shown evidence that supports the following four path ways: exocytosis, hemi-channels, anion transporters, and P2X receptors, among which an exocytotic mechanism is highly emphasized (Haydon and Carmignoto, 2006). Since effective release from hemi-channels and $P2X_7$ receptors requires the presence of low divalent saline, in an astrocyte, with normal level of divalent action, the open probability of hemi-channels and of $P2X_7$ receptors is so low, thus these pathways are unlikely to be utilized in physiological conditions. So far, the detailed function of anion transporters is still unknown due to the poor selectivity of antagonists. Nevertheless, research has been done showing a possibility that this pathway may contribute to the release of glutamate from the astrocyte (Kimelberg et al, 1990).

1.4.2. Calcium mediated glutamate release and exocytosis

Today, supporting evidence for an exocytotic mechanism of glutamate release from astrocytes is compelling. Exocytosis is the functional process. The cell directs the contents of secretory vesicles into the cell membrane. These membrane-bound vesicles contain soluble proteins to be secreted to the extracellular environment, as well as membrane proteins and lipids that are sent to become components of the cell membrane (Figure 1.4).

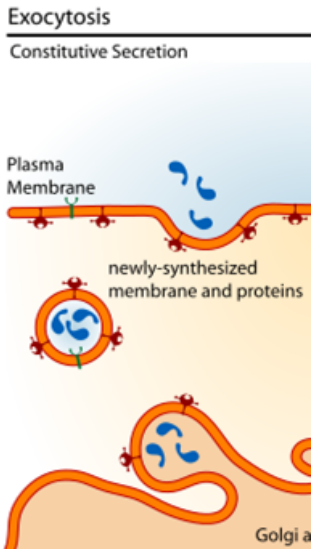

Figure 1.4. Illustration of an exocytotic mechanism of glutamate release from astrocytes (Hill M, Cell Biology course, The University of New South Wales, Sydney, Australia. Access date: Apr. 22, 2009)

Exocytosis in synapses is Ca^{2+} triggered and results in an interneuronal signaling. The whole exocytosis process involves vesicle trafficking, vesicle tethering, vesicle docking, vesicle priming, and vesicle fusion. Some vesicle proteins expressed in glial cells are important for exocytosis. It is known that if clostridial toxins, which can cleave target SNARE proteins, are introduced into the astrocytes, glutamate release can be reduced (Araque et al., 2000). Research work using expression of VGLUT-EGFP fusion proteins as well as acridine orange (AO) done by Volterra and colleagues (Bezzi et al., 2004) using total internal reflection fluorescence microscopy are consistent with regulated exocytosis in astrocytes. Furthermore, exocytotic release of this gliotransmitter from astrocytes is also strongly supported by the observation that cocultured glutamate receptor expressing reporter cells can simultaneously detect the release of glutamate.

After the discovery of the regulated release of glutamate from astrocytes, attention has been directed to demonstrate that this gliotransmitter can modulate synaptic

transmission and neuronal excitability. Results from cell culture studies support these findings, which clearly showed the potential for astrocytes to integrate neuronal activity and to provide feedback signals for modulation.

Astrocytic calcium waves can cause the calcium-dependent release of glutamate. It is known that neuronal activity and transmitters can evoke elevations of astrocytic Ca^{2+}, which was introduced earlier in this thesis. The release of these neurotransmitters, which in fact, can also be released from glia, is also Ca^{2+}-dependent. Ca^{2+} elevations are necessary and sufficient to induce glutamate release from astrocytes, which is seen in experiments in which the release of glutamate from astrocytes in cell culture was visualized using an enzymatic assay. In the presence of the cofactor NAD^{+} and the enzyme glutamate dehydrogenase in the bathing solution, glutamate released from astrocytes is converted to α-ketoglutarate and NAD^{+} (Nicotinamide adenine dinucleotide) is reduced to NADH. As NADH is fluorescent, it is possible to image the presence of glutamate using fluorescence microscopy (Haydon, 2001). This Ca^{2+}-dependent glutamate release can be detected both in purified astrocytes in cell culture and in astrocytes in normal brain tissue.

1.4.3. Neuron - glia interactions

The unique morphology of astrocytes enables them to sense transmitters released from neurons and other astrocytes. Astrocytes exhibit a large number of GPCRs, and these receptors can be activated by neurotransmitters released from presynaptic terminals. This finding demonstrates the existence of neuron-astrocyte communication, in which astrocytic GPCRs could be a primary link between neuronal activity and astrocytic Ca^{2+}

elevations. Research evidence for a reciprocal effect of astrocytes on synaptic transmission through the Gq GPCR mediated Ca^{2+}-dependent release of neuroactive molecules (called gliotransmitters), raises the possibility that astrocytes not only listen and react to ongoing neuronal activity, but also have the ability to modulate this activity via the release of gliotransmitters.

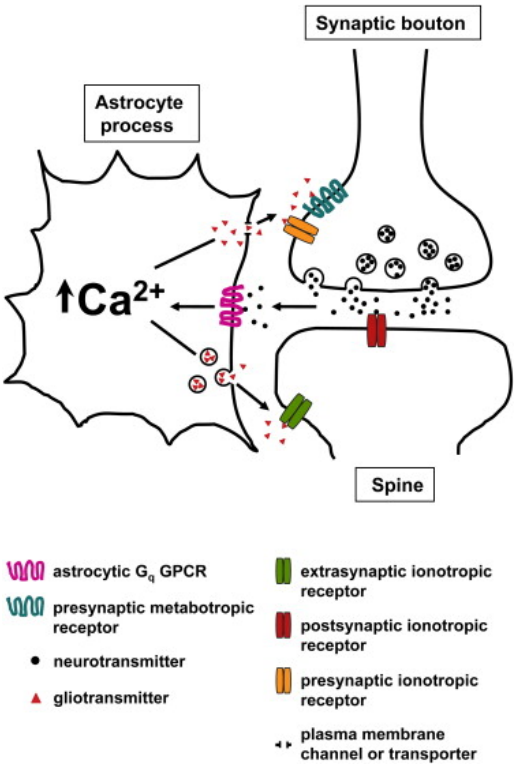

Figure 1.5. Schematic depicting the tripartite synapse. The presynaptic and postsynaptic compartments together with the enveloping astrocytic process form the tripartite synapse. Neurotransmitters released from presynaptic terminals act on postsynaptic receptors and astrocytic Gq GPCRs following spillover from the synaptic cleft. Astrocytic Gq GPCR-mediated Ca^{2+} elevations may trigger the release of gliotransmitters through unresolved pathways. Astrocyte-released gliotransmitters may then signal back to neurons by activating presynaptic or postsynaptic (extrasynaptic) neuronal receptors to modulate synaptic transmission. (Agulhon et al., 2008)

Recent studies indicate the concept of the "tripartite synapse" (Figure 1.5), in which the process of an astrocyte wraps around a synaptic connection. Synaptic release of GABA or glutamate can act on astrocytic receptors and trigger IP_3-dependent Ca^{2+} release from internal stores to increase cytosolic astrocytic Ca^{2+} levels. Elevated astrocytic Ca^{2+} evokes the local release of chemical transmitters such as glutamate, which can modulate the synapse. This is basically the whole idea about the interaction between

neurons and astrocytes. Thus, astrocytes, in addition to pre- and post-synaptic functions, are functional components of the synapse (Agulhon et al., 2008).

1.5. Astrocytes in ischemic stroke

Ischemia is defined as abolished or reduced blood supply to an organ. Ischemic stroke is caused by a transient or permanent reduction in cerebral blood flow which is restricted to the territory of a major brain artery. The cause of this reduction in flow is usually the occlusion of a cerebral artery either by an embolus or by local thrombosis. The incidence of stroke is approximately 250-400 in 100,000 with a mortality rate of around 30%, which makes it the third leading cause of death in industrialized countries. The USA, for example, has four million survivors coping with the debilitating consequences of stroke (Dirnagl et al., 1999). The prevalence of stroke makes it extremely important to inform patients about the early symptoms, as well as to find a successful treatment. Our work will contribute to understanding the relationship between astrocytic Ca^{2+} signaling and neuronal death following ischemia stroke.

1.5.1. Ischemic cell damage and the glutamate hypothesis

Because of the loss of energy supply, glucose triggers a series of events and each step takes some time. Thus, the neurons often do not die until several hours after the ischemic episode, but eventually ischemia results in massive neuronal death. Glutamate excitotoxicity is the principal mechanism that causes brain damage. Excitotoxicity is the pathological process by which nerve cells are damaged and even killed by glutamate or similar substances. Following an increase of astrocytic Ca^{2+}, Ca^{2+}-mediated glutamate

release from astrocytes occurs through an exocytotic mechanism, which was described earlier in this thesis. At high levels of glutamate, many receptors such as the NMDA receptor and AMPA receptor can be overly activated. Excitotoxins like NMDA and kainic acid which bind to these receptors, can cause excitotoxicity by allowing high levels of Ca^{2+} to enter the cell (Manev et al., 1989). Ca^{2+} influx into cells activates a number of enzymes, including phospholipases, endonucleases, and proteases. These enzymes damage cell structures such as the cytoskeleton, membrane, and DNA. Excitotoxicity may be involved in spinal cord injury, stroke, traumatic brain injury and neurodegenerative diseases of the central nervous system. The following diagram depicts the sequence of events following ischemia (Brodal, 1998):

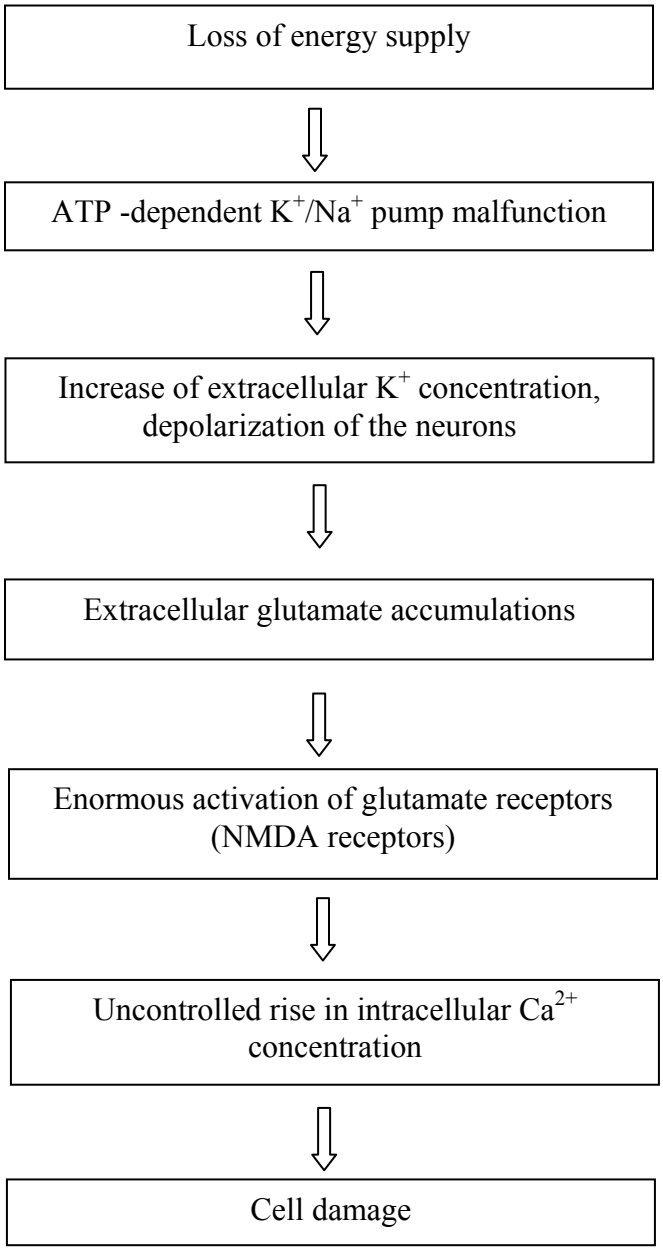
Loss of energy supply
ATP -dependent K^+/Na^+ pump malfunction
Increase of extracellular K^+ concentration, depolarization of the neurons
Extracellular glutamate accumulations
Enormous activation of glutamate receptors (NMDA receptors)
Uncontrolled rise in intracellular Ca^{2+} concentration
Cell damage

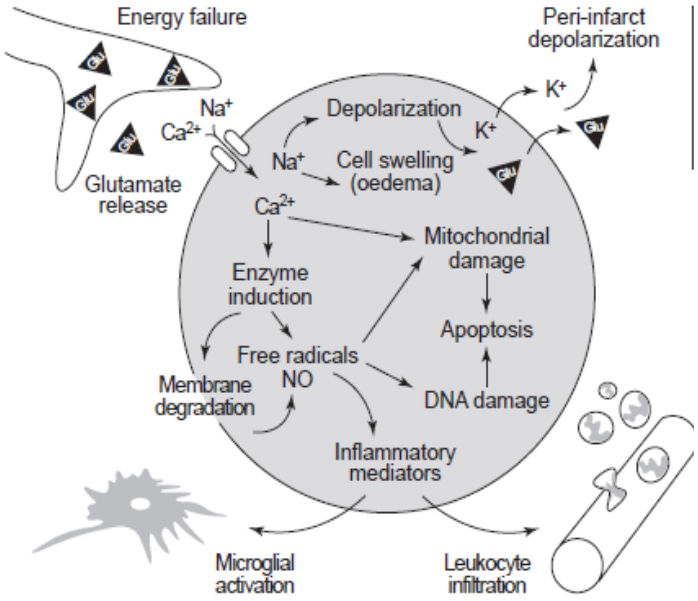

Figure 1.6. An overview of pathophysiological mechanisms in the focally ischaemic brain. Energy failure leads to the depolarization of neurons. Activation of specific glutamate receptors dramatically increases intracellular Ca^{2+}, Na^{+}, Cl^{-} levels while K^{+} is released into the extracellular space. Diffusion of glutamate (Glu) and K^{+} in the extracellular space can propagate a series of spreading waves of depolarization (peri-infarct depolarizations). Water shifts to the intracellular space via osmotic gradients and cells swell (oedema). The universal intracellular messenger Ca^{2+} overactivates numerous enzyme systems (proteases, lipases, endonucleases, etc.). Free radicals are generated, which damage membranes (lipolysis), mitochondria and DNA, in turn triggering caspase-mediated cell death (apoptosis). Free radicals also induce the formation of inflammatory mediators, which activate microglia and lead to the invasion of blood-borne inflammatory cells (leukocyte infiltration) via upregulation of endothelial adhesion molecules (Dirnagl et al., 1999)

Figure 1.6 provides a similar description of this mechanism, which explained a series of events following after energy depletion caused by focal impairment of cerebral blood flow.

This glutamate hypothesis can not readily explain all aspects of ischemic cell death. For example, after global ischemia, the cell death is not diffusely distributed. The neurons in the CA1 field of the hippocampus are highly vulnerable and this can not be simply explained as regional differences in glutamate release or glutamate receptors distribution.

It is more likely because of differences among regions regarding the presence and regulation of neurotrophic factors. The delay between an ischemic episode and irreversible cell damage has become an active field of research, since it gives hope for finding drugs that prevent or reduce the brain damage.

1.5.2. Does Ca^{2+}-dependent glutamate release from astrocytes contribute to neuronal death?

As described earlier in this thesis, glutamate release from astrocytes is Ca^{2+}-dependent. This glial source of glutamate has the potential to cause neuronal excitotoxicity since the activation of extrasynaptic NMDA receptors has been shown to activate the neuronal cell death path way (Ding et al., 2007).

After stroke, the first phase of rapid improvement will last from days to weeks, and then the second phase slower progress can last from months to years. Acute damage to neural tissue will cause secondary changes in the tissue surrounding the damaged area, such as disturbed local circulation and tissue swelling, which is also known as an inflammatory reaction. All of these result in a weaker and slower immune reaction in the CNS. Thus, neurons outside the damaged region may be temporarily or permanently out of function. The main task of astrocytes after injury is to strengthen their normal function of keeping the extracellular fluid composition constant. Tissue damage increases the flow of ions and transmitters from the neurons to the extracellular fluid. Astrocytes increase their uptake to counteract such disturbances of the neuronal environment. Since the substances taken up are osmotically active, the astrocytes can swell very quickly. This may contribute to brain edema, which is a dangerous complication after head injuries. In

the long term, astrocytes produce a kind of scar tissue at sites where neurons are lost (Brodal, 1998).

Our previous work shows that astrocytes exhibit enhanced Ca^{2+} signaling after photothrombosis-induced ischemic stroke model on living mice (Figure 3.1 in Results and Discussions), raising the possibility of the potential role of glial glutamate in neuronal death and brain damage. However, whether Ca^{2+}-dependent glutamate release from astrocytes contributes to neuronal death and brain damage after ischemia has not been studied.

1.6. Aims of this project

In this work, we focused on one of the subtypes of glial cells, astrocytes, how astrocytic Ca^{2+} affects ischemic brain injury. Based on previous studies, our goal was to test the hypothesis that inhibition of astrocytic Ca^{2+} will ameliorate neuronal damage through the reduction of glutamate release from astrocytes. We had two aims to test this hypothesis:

Aim 1: We will use BAPTA-AM to chelate Ca^{2+} in astrocytes to determine its effects on neuronal death after ischemia.

Aim 2: We will use genetic manipulation to study the effect of IP_3-dependent Ca^{2+} signaling pathway on ischemic injury. We will express p130PH protein to disrupt IP_3-dependent Ca^{2+} signaling pathway. In this approach, we will conduct our experiments on cultured astrocytes as well as *in vivo* study on a mouse model:

1) We will test whether p130PH expression will inhibit Ca^{2+} signaling in cultured astrocytes using both primary cultured astrocytes and an astrocyte cell line. We will

introduce p130PH into astrocytes by cell transfection to inhibit the IP_3 pathway and test its effect on astrocytic Ca^{2+} signaling.

2) We will develop recombinant adeno-associated viral (rAAV) vectors that can specifically introduce transgenes into astrocytes. pZac2.1-ABC1D-mRFP-p130PH plasmid that contains both an astrocyte-specific promoter ABC1D and p130PH gene was used for *in vivo* study (positive group).

3) Finally, we will examine the transgene expression in astrocytes *in vivo* after viral transduction using immunocytochemistry. Within this step, we will transduce mouse cortex with rAAV vector to introduce p130PH protein into the brain, then examine p130PH expression patterns in mouse brain. After assurance of the target gene expression, we will move on to study the effects of this IP_3-inhibitor on ATP stimulated astrocytic Ca^{2+} signaling. Our long term goal is to examine whether inhibition of Ca^{2+} in astrocytes by p130PH will reduce neuronal death and brain damage following ischemia *in vivo*.

It is believed that astrocytes are involved in pathogenesis in brain injury after ischemia and astrocytes mediate glutamate release in response to Ca^{2+} elevations. Our research, by using these molecular approaches, will eventually reveal its relevance to the brain damage caused by ischemia.

CHAPTER 2

METHODS AND MATERIALS

2.1. Cultured astrocytes

Preparation of cover slips: A whole cover slip (24x50 mm, Fisher Scientific, PA) was cut into small pieces (0.5 cm^2). They were first washed with 70% ethanol (ethanol from Aaper, KY), and subsequently with sterile double-distilled water (dd H_2O) five times. All the cover slips were placed into a clean beaker covered with Al foil, autoclaved for 30 minutes at 121°C and dried for 30 minutes. The beaker was stored in a biological safety cabinet (Thermo, MS).

Cell split: Primary cortical astrocytes (kindly provided by Dr. Grace Y. Sun's lab, Department of Biochemistry, University of Missouri) from newborn rat brains were prepared using a standard stratification/cell-shaking procedure (McCarthy and Vellis, 1980). This procedure yielded confluent mixed glial cultures within 7–9 days, after which the flasks were rotated at 180 rpm at room temperature (15-25°C) for 3 hours to remove microglial cells. Then the cells were cultured in a 25 cm^2 cell culture flask (Corning, NY) with a slightly modified Dulbecco's medium (Dulbecco's modified eagle medium (DMEM), high glucose 1x), Invitrogen, MI) containing 10% (vol/vol) fetal bovine serum (FBS) (Atlanta Biologicals, GA) and 1% (vol/vol) penicillin-streptomycin (Invitrogen Corporation, MI).The medium was changed every two days after inoculation. Before splitting, cells were examined under the microscope to determine the split ratio. Two mL 1x Dulbecco's phosphate buffered saline (DPBS) (Invitrogen Gibco, IN) was added to

rinse the cells. The flask was gently rotated and then DPBS was aspirated. Two mL 1x 0.05% trypsin-EDTA (Invitrogen, MI) was then added and gently mixed around the plate. The flask was placed in a 37°C 5% CO_2 incubator (Heracell 150, Heraeus, IN) for 1.5-2 minutes, during which a new 24 well tissue culture plate (Multiwell, BC) was prepared by adding one 0.5 cm^2 cover slip per well. The cells in the flask were mixed gently with DMEM by pipette. Cells were then dispensed (600 μL cell/medium mixture for each well) to the new 24 well tissue culture plate. The plate was placed back into the 37°C 5% CO_2 incubator.

Cell transfection: Plasmid pC1 with transgene p130PH-mRFP (i.e., p130PH fused with marker protein mRFP) was kindly provided by Dr. Gyorgy Hajnoczky (Thomas Jefferson University, PA). For the control experiment, mRFP with Age I at the 5' end and EcoR I at the 3' end was amplified using PCR and ligated with pC1 plasmid to produce plasmid pC1-mRFP. Astrocytes were transfected with plasmid pC1-mRFP-p130PH or pC1 -mRFP (control group) one day after cell splitting. For a 35 mm dish with 4 cover slips, 150 μL serum free DMEM was added to a 1.5 mL sterile microcentrifuge tube (Fisher Scientific, PA) and 4.5 μL FuGENE 6 transfection reagent (Roche Diagnostics, IN) was then added. They were gently mixed with the medium by tapping the tube. The tube was incubated at room temperature for 5 minutes, while being tapped every one minute. Plasmid DNA (1.5 μg) was added into a second tube. The mixture in the first tube was added to the DNA tube and mixed gently by tapping the tube. The mixture was incubated for 30 minutes at room temperature. After the medium was changed, cells were

transfected by adding FuGENE 6 transfection reagent/DNA mixture dropwise to the plate wells.

2.2. Calcium imaging in cultured astrocytes

Ca^{2+} imaging was performed one day after transfection using an upright wide-field epi-fluorescence microscope (FN1 system, Nikon) with 40x/0.8 water immersion objective. Astrocytes were examined under the microscope to determine if they were in good condition. One 0.5 cm^2 cover slip was picked out and incubated (in dark) with 0.5 mL Ca^{2+} indicator fluo-4, AM (Invitrogen Molecular Probes, OR) (1 μg/ml, diluted from a stock solution of 1 μg/μl prepared with dimethyl sulfoxide (DMSO)) in artificial cerebral spinal fluid (ACSF): 120 mM NaCl, 10 mM Hepes, 3.1 mM KCl, 2 mM $CaCl_2$, 1.3 mM $MgCl_2$, and 10mM glucose, pH 7.4. All chemicals were purchased from Sigma. Forty-five minutes later, the cover slip was placed into the chamber and fluo-4, AM was washed away with ACSF using a perfusion system with ACSF solution, which can be controlled by a pinch valve. Excitation was generated by an X-Ford metal halide lamp filtered with a fluo-4 filter cube. Emission was detected by a CoolSNAP-EZ CCD-camera (Photometrics, AZ). The red fluorescence was excited by the lamp with a yellow excitation filter (Y-2E/C filter combination, Nikon, NY. Excitation filter wavelengths: 540-580 nm), and the green fluorescence was excited by the lamp with a blue excitation filter (B-2E/C filter combination, Nikon, NY. Excitation filter wavelengths: 465-495 nm). Fluorescent images were acquired using Metamorph imaging software (Universal Imaging, CA). Time lapse imaging was performed to track Ca^{2+} signals for a period of 5 minutes with acquisition rates of 1 image in every 2 seconds. ATP (20 μM, Invitrogen

Molecular Probes, OR) was added at the 20th frame to stimulate the astrocytes for 20 seconds, and washed away by switching to the ACSF solution afterwards. The coverslips were perfused with ACSF for at least 10 minutes between two time-lapse imaging to completely wash away ATP. All the documents were saved for analysis. For each cover slip, 15-25 astrocytes in 3-4 fields were imaged and 5-8 coverslips were used for each experimental condition.

2.3. Molecular biology

2.3.1. Construction of DNA plasmid for rAAV vectors

Plasmid pZac2.1-ABC1D: To construct a *cis* expressing plasmid that has an astrocyte specific GFAP promoter and gene of interest, the CMV promoter of the *cis* cloning plasmid pZac2.1 was swamped by a 681 bp GFAP promoter gfaABC$_1$D (a plasmid containing gfaABC$_1$D promoter was kindly provided by Dr. Michael Brenner, University of Alabama, AL) using Bgl II (Fisher Scientific, PA) on the 5' end and EcoR I (Fisher Scientific, PA) on 3' end. Two restriction enzyme reaction systems were set:

Plasmid pgfa-ABC1D was digested with Bgl II and EcoR I at 37°C for 3 hours to cut off the gfaABC1D promoter:

EcoR I	10 μL
Bgl II	5 μL
10x Buffer D	10 μL
BSA	10 μL
DNA	13.6 μL (10 μg)
dd H_2O	51.4 μL
Total	100 μL

Plasmid pZac2.1 was digested with Bgl II and EcoR I at 37°C for 3 hours to remove the CMV promoter in the original plasmid:

EcoR I	10 µL
Bgl II	5 µL
10x Buffer D	10 µL
BSA	10 µL
DNA	12.9 µL (10 µg)
dd H_2O	52.1 µL
Total	100 µL

The results of the enzyme digestion (amount and size of DNA) were roughly detected by DNA Gel electrophoresis (0.8% electrophoresis gel: 0.4 g agarose, Fisher Bioreagents, PA; 40 mL dd H_2O; 10 mL 5x electrophoresis buffer (1 L 5x electrophoresis buffer: 24.2 g tris base; 5.71 mL glacial acetic acid; 0.5 M EDTA; pH 7.6) with 25 µL ethidium bromide, Acros Oganics, NJ; DNA loading dye: 1:6 (vol/vol), Promega, WI; 1 kb DNA ladder (0.05 µg/mL), Fisher Scientific, PA). After extraction of DNA from the gel, a ligation reaction was set up to ligate the promoter gfaABC1D with the *cis* cloning plasmid pZac2.1:

Plasmid DNA	1.6 µL (200 ng)
Insert DNA	8.9 µL (400 ng)
10x Ligase Buffer	2.5 µL
T4 DNA Ligase	1.5 µL
dd H_2O	10.5 µL
Total	25 µL

The mixture was incubated at 14°C overnight for ligation. T4 DNA ligase was purchased from New England Biolabs, MA. Ligation products were transformed into

XL1-Blue supercompetent cells (Stratagene, TX) following the instruction for the protocol. Colonies grown on Luria-Bertani (LB) broth dishes (LB medium: 20 g LB broth Sigma, MO; 1 L dd H_2O, 15 g agar, Fisher Scientific, PA) with 100 μg/mL ampicillin (Sigma, MO) were picked and inoculated into the tubes with 2 ml LB liquid medium each. After 16-18 hours, mini preparation of DNA was done according to the instruction of PureLinkTM Hipure Plasmid Filter Purification kits (Invitrogen™, MI). The DNA obtained, namely pZac2.1-ABC1D, was first tested by Sma I enzyme digestion and further with DNA sequencing to confirm the correct insertion.

pZac2.1-ABC1D-mRFP-p130PH: In order to insert transgene p130PH with fusion protein mRFP into pZac2.1-ABC1D, namely plasmid pZac2.1-ABC1D-mRFP-p130PH, we used polymerase chain reaction (PCR) to generate EcoR I sites at both 5'- and 3'-terminals from a original template DNA vector pC1-mRFP-P130PH (provided by Dr. Gyorgy Hajnoczky, Thomas Jefferson University, PA) by mutating the 5' end from an Age I cutting site into an EcoR I cutting site, while maintaining the 3' EcoR I cutting site and 3' end.

PCR reaction system:

Template DNA	3 μL (100 ng)
dNTP mixture	12.5 μL (400 ng)
5' primer	1.5 μL (100 ng/μL)
3' primer	1.5 μL (100 ng/μL
10x Pfu Ultra II Buffer	10 μL
Pfu Ultra II DNA Polymerase	1 μL
dd H_2O	70.5 μL
Total	100 μL

PCR reaction cycle:

95°C	2 min	
95°C	30 sec	25x
54°C	30 sec	
68°C	1 min 30 sec	
68°C	7 min	
4°C	∞	

Primers for PCR reaction were designed as following:

P1 (5' primer):
5'-GCCGAATTCCGCCACCATGGCCTCCTCCGAGGAC-3'
P2 (3' primer): 5'-
GCCGAATTCACATAAAGTCAAGTGGTTGCTTACTGCGAGAGAC-3'
dNTP (Fisher Scientific, PA); Pfu Ultra II DNA Polymerase (STRATAGENE, TX)

PCR products were digested with EcoR I, purified and then inserted into linearized pZac2.1-ABC1D with EcoR I to form a new expressing plasmid pZac2.1-ABC$_1$D-p130PH-mRFP. PCR product with mRFP-p130PH fragment was digested with EcoR I at 37°C for 3 hours in the following reaction system:

EcoR I	1 μL
10x Buffer H	10 μL
BSA	10 μL
DNA	50 μL
dd H_2O	29 μL
Total	100 μL

Plasmid pZac2.1-ABC1D was linearized with EcoR I at 37°C for 3 hours in the following reaction system:

EcoR I	1 μL
10x Buffer D	10 μL
BSA	10 μL
DNA	15 μL
dd H_2O	64 μL
Total	100 μL

Two μL shrimp alkaline phosphatase (SAP) (Promega, WI) was added into the reaction system and incubated at 37°C for another 15 minutes. SAP was then inactivated by heating to 65°C for 15 minutes. The results of the enzyme digestion (amount and size of DNA) were roughly detected by DNA gel electrophoresis. After extracting DNA from the gel, a ligation reaction was set up to ligate the transgene mRFP-p130PH with the linearized plasmid pZac2.1-ABC1D. A control group was also set up with only linearized plasmid pZac2.1-ABC1D, but no DNA inserts to examine the background effects from plasmid pZac2.1-ABC1D. The reaction mixtures were incubated at 14°C overnight.

Ligation reaction system:

Plasmid DNA	1 μL (200 ng)
Insert DNA	3.5 μL (400 ng)
10x Ligase Buffer	1 μL
T4 DNA Ligase	0.5 μL
dd H_2O	4 μL
Total	10 μL

Ligation reaction system (control group):

Plasmid DNA	1 μL (200 ng)
10x Ligase Buffer	1 μL
T4 DNA Ligase	0.5 μL
dd H_2O	7.5 μL
Total	10 μL

Ligation products were transformed into XL1-Blue supercompetent cells (Stratagene, TX) following the instruction of the protocol. Colonies that grew on the LB dish with 100 μg/mL Ampicillin (Sigma, MO) were picked up and mini preparation of the DNA was done according to the instruction of PureLink Hipure plasmid filter purification kits (Invitrogen, MI). DNA was first roughly tested by Sma I enzyme digestion. The construct was further sequenced to confirm the correct insertions of promoter and transgene.

Plasmid with only with report gene mRFP under the control of ABC1D promoter, namely, pZac2.1-ABC1D-mRFP, was constructed in a similar approach using PCR for the control experiment.

Cell transformation: Two 14 mL BD Falcon polypropylene round-bottom tubes (Fisher, PA) were pre-chilled on ice (one tube is for the experimental transformation and one tube is for the control). Super Optimal broth with catabolite repression (SOC medium: SOB with added glucose) (Mediatech Cellgro, VA) was preheated to 42°C. XL1-Blue supercompetent cells (Stratagene, TX) were thawed on ice. After thawing, 50 μL cells were gently mixed and applied to each of the two pre-chilled tubes. A 1.7 μL β-mercaptoethanol provided with the kit was added into each aliquot of cells. The contents of the tubes were gently swirled and then the cells were incubated on ice for 10 minutes,

while being gently swirled every two minutes. Approximately 0.1-50 ng DNA (5-10 μL ligation products) was applied to one aliquot of cells (the same for the control group). The tubes were gently swirled and then incubated on ice for 30 minutes. Heat-pulse was done in a 42°C water bath for 45 seconds. The duration of the heat pulse is critical for maximum efficiency. Tubes were then put on ice for two minutes. Preheated SOC medium (900 μL) was added and tubes were incubated at 37°C for 1 hour with shaking at 225-250 rpm. The transformation mixture (200 μL) was spread on the LB dish containing 100 μg/mL ampicillin. Cells may be concentrated by centrifuging at 1000 rpm for 10 minutes and resuspending the pellet in 200 μL of SOC medium. LB dishes were incubated at 37°C overnight.

DNA precipitation: The volume of the DNA solution was estimated and according to which sodium chloride was added to reach a final concentration of 0.2 M. We added exactly 2 volumes of ice-cold 100% ethanol (Pharmco-Aaper, KY) and again mixed the solution well. The ethanolic solution was stored on ice for at least 1 hour (overnight in the refrigerator is preferred) to allow the DNA precipitate to form. DNA was recovered by centrifuging at 0°C (maximum speed: 100,000g) for 20-30 minutes. The supernatant was carefully removed with a micropipette so as not to disturb the pellet of nucleic acid, which may be invisible. The supernatant from the DNA samples was saved until recovery of the precipitated DNA has been verified. Around 500 μL 70% ethanol was added. The tube was centrifuged at the maximum speed for 5 minutes at 4°C. The supernatant was carefully removed with a micropipette. The tube was kept open and stored on the bench at room temperature until the last traces of fluid had evaporated. The DNA pellet (which

is often invisible) was dissolved in the desired volume of buffer (30-50 μL ddH_2O) and kept at 4°C for later use.

***DNA preparations*:** DNA mini preparation, DNA maxi preparation and endotoxin free DNA maxi preparation were performed using commercially available kits and protocols. DNA mini preparation: PureLink quick plasmid miniprep kit (Invitrogen, MI); DNA maxi preparation: PureLink HiPure plasmid filter purification kits (Invitrogen, MI); endotoxin free DNA maxi preparation: Endofree plasmid maxi mega, and giga kits (Qiagen, MD).

DNA gel extraction: The procedure was done according to the instruction of the gel extraction kit (Qiagen, MD). The DNA fragment was excised from the agarose gel with a clean, sharp scalpel. The size of the gel slice was minimized by removing extra agarose. The gel slice was then weighed in a colorless tube. Buffer QG was added into the tube at a 3:1 ratio (3 volumes of buffer to 1 volume of gel; 100 mg~100 μL). The tube was incubated at 50°C for 10 minutes (or until the gel slice had completely dissolved). To help dissolve the gel, vortex the tube every 2-3 minutes during the incubation. After the gel slice has dissolved completely, the color of the mixture is checked to make sure it is yellow (similar to buffer QG without dissolved agarose). If the color of the mixture is orange or violet, 10 μL of 3 M sodium acetate (pH 5.0) should be added to adjust the pH, and the color of the mixture will turn to yellow. If the size of the DNA fragments were <500 bp or were >4 kb, add 1 gel volume of isopropanol to the sample to increase the yield. A QIAquick spin column was then placed into a provided 2 mL collection tube.

The sample was loaded to the QIAquick column to let the DNA bind onto the membrane. The tube was centrifuged for 1 minute at room temperature. The maximum volume of the column reservoir is 800 μL (for sample volumes of more than 800 μL, simply load and spin again). Flow-through was discarded and the QIAquick column was placed back in the same collection tube. On half milliliter of buffer QG was added and the column was centrifuged for 1 minute. A 0.75 mL of buffer PE was added to wash the QIAquick column. The column was centrifuged for 1 minute. After discarding the flow-through, the column was centrifuged for an additional 1 minute at 13,000 rpm. The QIAquick column was placed into a clean 1.5 mL microcentrifuge tube, 50 μL elution buffer (EB) or dd H_2O was added to the center of the QIAquick membrane to elute the DNA. The column was kept at room temperature 1 minute and then centrifuged for 1 minute. The DNA was stored at -20°C for later usage.

2.4. rAAV injection in mouse brain

Preparations of rAAV vectors: rAAV vectors were produced by triple transfection of H293 at the University of Pennsylvania Gene Therapy Program Vector Core and have a titer of 8×10^{12} genomic copies (GC)/ml). Briefly, this *cis* plasmid was cotransfected with an AAV *trans* plasmid (AAV2/5) encoding serotype 2 AAV (AAV2) *rep* and serotype 5 AAV (AAV5) *cap* genes and an adenoviral helper plasmid in HEK 293 cells to produce pseudo-type rAAV2/5 vectors. The vectors were purified using a method based on buoyant density (cesium chloride) ultracentrifugation and collected in 5% glycerol in PBS (Fisher, 1997). Vectors were stored in aliquots at -80°C and thawed on ice before use.

Animals: Male FVB/NJ mice 5–7 weeks of age were purchased from the Jackson laboratory (Bar Harbor, MA). All procedures were performed in accordance with the NIH guide for the care and use of laboratory animals and were approved by the University of Pennsylvania and University of Missouri institutional animal care and use committee.

Mouse surgery: Before the surgery, the light should be turned on and the operating table cleaned. Mice were anesthetized with an intraperitoneal (i.p.) injection of ketamine/xylazine (130 mg/10 mg/ kg body weight) dissolved in artificial cerebral spinal fluid (ACSF). Once the mouse reached a surgical level of anesthesia, it was placed on a warm heating pad to maintain body temperature at 37°C for surgery. Small holes (0.2 mm in diameter) in the skull were made separately using a high speed drill over the somatosensory cortex at the coordinate of -0.8 mm from bregma and 2.0 mm lateral to the midline.

rAAV virus microinjection: Vectors were stored in aliquots at -80°C and thawed on ice before use. The tip of the micro pipette was made about 20 μm with a pipette puller under the microscope. The oil was backfilled into a micropipette with a needle and syringe (avoiding any bubbles). The top and o-ring was taken off and the micropipette was put through the top, o-ring, and then plunger. Be sure the back end of the pipette and white sleeve could match each other. Screw the top softly, neither too tight nor too loose. The empty button was used to drive the bubble in the tip out of the pipette, as well as to drive some oil out in order to leave some space for the plunge while filling the virus. (Fast

empty: empty + fill button 230 nL/s; Empty: empty button 92 nL/s; #5 had no effect on empty mode). One μL rAAV virus (Fast fill: fill + empty button 230 nL/s; Fill: fill button 92nL; depending on #5 positions) was filled into the micropipette. The micropipette was advanced into the cortex about 250 μm and controlled by the micromanipulator. One μL virus was injected into each hole (under mode UDUU for 9.2 nL each injection) by pressing the inject button. After injection, the micromanipulator was removed from the brain. The top was loosened and the oil was wiped off. Everything was cleaned up and put into the right position. The skin of the mouse was sutured and the mouse was put on the heating pad for post-surgery recovery. The mouse was returned to the animal facility after recovery from surgery.

2.5. Photothrombosis-induced focal cerebral ischemia model

To induce photothrombosis, the photosensitive dye Rose Bengal (RB) was dissolved in ACSF and injected through the tail vein at a dose of 0.03 mg/g body weight. To activate the dye, an area in the middle of the craniotomy was focally illuminated with a green light (535±25 nm) from a mercury lamp for 2 minutes through a 10 x 0.3NA objective. For the histological study we illuminated an area of 1 mm in diameter. For simplicity, the illuminated area was regarded as the ischemic core region, and the surrounding area the penumbra.

2.6. Immunohistochemistry

Mouse cardiac perfusion: For cardiac perfusion, mice were anesthetized with 2 - bromo - 2 chloro-1, 1, 1 – trifluoroethane (Sigma, MO). The thoracic cavity was opened to

expose the heart and ascending aorta. An 18-gauge needle connected to the collection tubing was inserted through the left ventricle into the ascending aorta. A pump was applied to slowly perfuse the mouse with about 40-50 mL 0.1 M PBS at room temperature (pH 7.4, 500 mL: NaCl 4.55 g; Na_2HPO_4 5.68 g; NaH_2PO_4 1.2 g; ddH_2O) until the fluid was clear**.** Then PBS was changed to freshly prepared ice-cold 4% paraformaldehyde (PFA) (dd H_2O 150 mL, paraformaldehyde 4 g, NaOH 0.7 g, NaH_2PO_4 2.4 g, pH 7.2-7.6). When the mouse's forelimbs were fully extended, the perfusion speed was reduced. When perfusion was complete, the mouse was decapitated and the brain was quickly removed using a caudal approach. The brain was placed in 4% PFA at 4°C for overnight as post fixation, and was moved to 30% sucrose at 4°C for another 24 hours.

Gel coating of glass slides: Before mounting the tissue, the glass slides must be gel coated. Fifty slides were loaded in each of six slide racks (300 in total). The slides were washed in a soapy container with hot water for approximately 1 hour. A 2.5 g gelatin (type A, Acros, IN) was added to the 500 mL pre-heated 70°C dd H_2O to make the gelatin solution. The solution was then added with 0.25 g chromium potassium sulfate (Fisher Scientific, PA) and stirred for 2-3 minutes until dissolved. The gel solution was poured into a glass container in an ice bucket and cooled to 4°C. The glass slides were quickly rinsed with deionized water (DI water) before soaking the slides in the gel solution. The slide racks were soaked in gel for 2 minutes and removed allowing the slides to dry for 5-10 minutes. Always store slides with the frosted side down, thus any

excess gel will accumulate on the frosted portion but not where the tissues will be. The racks (with frosted end down) were placed in an oven (70°C) overnight.

***Brain slice cutting with cryostat*:** Before cutting, the glass slides were labeled with the animal's ID, the section of the brain that is being sliced, the date of the experiment and the cryostat was set up to -22°C. A razor blade was used to cut the brain at the junction of the hindbrain and the forebrain to completely separate the forebrain from the hindbrain. The forebrain was placed on a small piece of foil (label the foil with the ID of the brain) and the foil and brain were put together in the cryostat to freeze. The brain needed to be in the cryostat for approximately 25-30 minutes before it could be sliced. While brain was freezing, a chuck was placed in the cryostat. DI water was applied to the chuck using a dropper. After the brain frozen, more water was added to the chuck and then the brain was placed on the chuck. The brain was positioned so that the caudal end (flatter) was down on the chuck and the rostral end (pointier) was up. More water can be added on and/or around the brain to stabilize it on the chuck. After all the water has frozen, the chuck was put on the cryostat. The brain was adjusted using the lever, and then the lever was tightened when the brain was positioned correctly. The guard was removed from the blade for slicing. Be sure to check the position of the brain in relation to the blade. The brain can be moved toward or away from the blade using the buttons on the top left of the cryostat. When slicing, a few slices before the injection point were saved; all of the slices that are within the injection point and a few slices after the injection point is gone were all saved. Once there were enough slices on the stage, one of the previously labeled slides was placed face down on the slices, and then picked up to stick slices to the slide. DI

water can be used to smooth bubbles or wrinkles out, if there are any in the slices. After smoothing out the slices, slides were placed in a slide book and dried for at least 24 hours before staining.

***Cresyl violet staining (Nissl staining*):** Slides were placed in alcohol : chroform (1:1) for 15 minutes, and allowed to dry slightly, before placing in 95% ethanol for 15 minutes. Slides were removed, dried slightly, and placed in 70% ethanol for 1 minute, and then rinsed with dd H_2O for 3 minutes and stained with cresyl violet solution for 2 minutes (0.2 % Cresyl Violet store solution: 0.2 mg into 100 mL dd H_2O. Two drops acetic acid was added to adjust the pH to 7.35. After mixing well, filtering and allowed to ripen for 48 hours, it is stable for 1 year). Slides were washed with dd H_2O for 2 minutes, placed in 70% ethanol for 2 minutes, then in 95% ethanol for 3 minutes and finally in 100% ethanol for 1 minute. Slides were placed in xylene for 5 minutes and were removed individually from the xylene bath by using forceps. Slides were placed flat on the table. A line of Permount mounting medium was applied along the bottom of the slide using a glass pipette. A coverslip was carefully placed on top of the Permount on the slide by touching one end of the slide and keeping the other end at a 45 degree angle, and was slowly lowered.

***GFAP staining*:** Brain slices were put into a 48 well plate (1section/well) with PBS and were kept in the refrigerator (4°C) before staining. While staining, brain slices were washed 3 times with 500 µL 0.1 M PBS at room temperature, each time, when the plate was placed on a shaker for 10 minutes. Brain slices were pre-blocked with 10% normal

donkey serum-triton-PBS (0.3% triton X-PBS: 300 μL triton into 100 mL PBS; 10% donkey serum-triton-PBS: 50 μL Donkey serum into 450 μL 0.3% Triton X-PBS) at room temperature on the shaker for 30 minutes. Slices were again washed 3 times with 500 μL 0.1 M PBS at room temperature, each time on a shaker for 10 minutes. Slices were incubated overnight in GFAP 1st antibody (rabbit anti-GFAP, Sigma, MO at a dilution of 1:160; 150 μl antibody solution per well)-1% normal donkey serum-triton-PBS (1% donkey serum-triton-PBS: 10 μL donkey serum into 990 μL 0.3% triton X-PBS). Slices were washed 3 times with 500 μL 0.1 M PBS at room temperature on a shaker (10 minutes each time). Slices were incubated in the dark for 2-4 hours with a 2nd antibody (FITC-conjugated goat anti-rabbit IgG second antibody, Chemicon, IL; ratio: 1:200; 150 μl antibody solution per well)-1% normal donkey serum-triton-PBS, then were washed 3 times with 500 μL 0.1 M PBS at room temperature, each time on the shaker for 10 minutes. Brain slices were sealed with anti-fade Permount in dark and were stored at 4°C.

Similar procedures were used for NeuN and Iba 1 staining. NeuN 1st antibody (mouse anti-NeuN monoclonal antibody, Millipore, FL; ratio: 1:1000; 150 μl antibody solution per well)-1% normal donkey serum-triton-PBS (1% donkey serum-triton-PBS: 10 μL donkey serum into 990 μL 0.3% triton X-PBS) and 2nd antibody (goat anti-mouse IgG second antibody, Chemicon, IL; ratio: 1:200; 150 μl antibody solution per well)-1% normal donkey serum-triton-PBS were used for neuronal staining. Iba1 1st antibody (rabbit anti-Iba1 polyclonal antibody, Wako Pure Chemical Industries, VA; ratio: 1:600; 150 μl antibody solution per well)-1% normal donkey serum-triton-PBS (1% Donkey

serum-triton-PBS: 10 μL donkey serum into 990 μL 0.3% triton X-PBS) and 2nd antibody (FITC-conjugated goat anti-rabbit IgG second antibody, Chemicon, IL; ratio: 1:200; 150 μl antibody solution per well)-1% normal donkey serum-triton-PBS were used for microglia staining. Brain slices were sealed with the anti-fade Permount in the dark and were stored at 4°C.

CHAPTER 3

RESULTS AND DISCUSSION

3.1. Previous study: Astrocytes exhibit enhanced calcium signaling in astrocytes following ischemia

In our previous study, we found astrocytes exhibited enhanced Ca^{2+} signaling after photothrombosis-induced ischemia using *in vivo* two-photon (2-P) Ca^{2+} imaging (Ding et al., 2009). We used fluo-4 AM to load cortical astrocytes, which was further confirmed by SR101, an astrocyte-specific fluorescent dye (Figure 3.1 A). Repetitive and transient Ca^{2+} signals in astrocytes were observed within 20 minutes after photothrombosis (RB+/Illumination+, Figure 3.1 C and D). We also noticed that Ca^{2+} signals exhibited a high degree of synchrony among astrocytes in the same imaging field (Figure 3.1 D). Photothrombosis not only increased the amplitude but also the frequency of Ca^{2+} signals. The development of Ca^{2+} signals in astrocytes was time-dependent and they were sustained for the duration of the imaging period up to 3 hours (Figure 3.1 F).

Our previous study also demonstrated that the increased frequency of transient Ca^{2+} signals after photothrombosis was not caused by 2-P excitation, green light illumination or RB *per se* (Figure 3.1 E). First, we performed Ca^{2+} imaging without RB injection and illumination (RB-/Illumination-) of the cortex. Second, Ca^{2+} imaging was performed after RB injection but without green light illumination of the cortex (RB+/Illumination-). Finally, Ca^{2+} imaging was performed after illumination in the absence of RB injection (Illumination+/RB-). Stimulation of Ca^{2+} signals required the combination of RB and green light illumination (Figure 3.1 E and F). These results are consistent with other

reports indicating that astrocytic Ca^{2+} signaling events are rare in normal anesthetized mice (Ding et al., 2007; Takano et al., 2006; Wang et al., 2006).

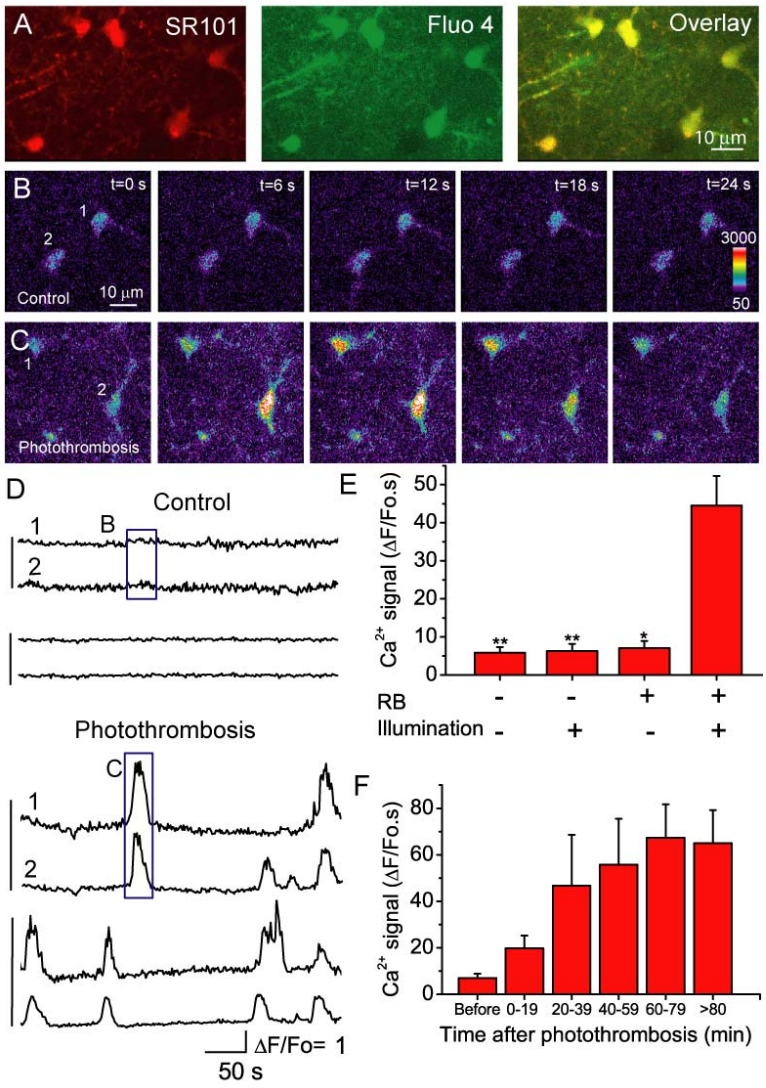

Figure 3.1. Astrocytes exhibit enhanced Ca^{2+} signals after photothrombosis. **(A)**. Cortical astrocytes double-labeled with fluo-4 and SR101 after photothrombosis. (**B**)-(**C**) Representative images of astrocytes loaded with fluo-4 before (**B**) and after (**C**) induction of photothrombosis. (**D**) Time course of somatic Ca^{2+} oscillations of astrocytes expressed as ΔF/Fo before (upper) and after (bottom) induction of photothrombosis. The vertical lines at the left indicate cell pairs that were recorded in the same image frame. The box regions correspond to the images in B and C as indicated. (**E**) Summary of astrocytic Ca^{2+} signals expressed as an integral of ΔF/Fo traces over 300 s under different control conditions and following photothrombosis (RB+ and Illumination+). The data were collected 20-80 min after ischemia from N=4-9 mice. Statistical analyses between photothrombosis (RB+/illumination+) and each control condition (i.e. RB-/Illumination-, RB-/Illumination+ and RB+/Illumination-) were assessed using *t*-test. *p<0.05, **p<0.01. (**F**) Time course of somatic Ca^{2+} signal in astrocytes developed after photothrombosis. The data from each time interval of 20 min were averaged from 14-28 cells obtained from N=4-5 animals. The Ca^{2+} signal of the last bin was the average value from astrocytes imaged 80-150 min after photothrombosis.

3.2. BAPTA-AM reduces ischemia-induced brain damage

As discussed earlier in the introduction, astrocytes have been shown to release glutamate in response to Ca^{2+} elevation. Glutamate excitotoxicity is a major mechanism that causes neuronal death and brain damage; however, the glutamate might be from multiple sources in brain tissue. In order to test the hypothesis that Ca^{2+}-dependent glutamate release from astrocytes after ischemia contributes to neuronal damage, specific astrocyte Ca^{2+} inhibition is required. In our previous study we demonstrated that cortical surface loading with BAPTA AM can selectively inhibit the ATP-induced Ca^{2+} signals in astrocytes, but not spontaneous neuronal Ca^{2+} signals (Ding, et al., 2007). Based on these results, we determined if BAPTA can reduce neuronal death following ischemia. We bilaterally induced photothrombosis in barrel cortices in the mouse brain, and subsequently applied premelted agarose containing 200 μM BAPTA AM onto one of the cranial windows to ensure continued delivery of BAPTA AM after photothrombosis. For the other side of the cranial window, we applied premelted agarose without BAPTA AM window to serve as a within-animal control. I perfused the mouse one day after ischemia, sectioned, and stained with cresyl violet. Then we measured infarct volumes to assess the effect of BAPTA AM on brain damage. As shown in Figure 3.2 A and B, infarction is well demonstrated in the presence or in the absence of BAPTA. Figure 3.2 C shows that selective loading of the Ca^{2+} chelator BAPTA AM into astrocytes reduces the infarct volume by 47% (N = 6 mice), indicating the neuronal protective role of BAPA-AM after ischemia.

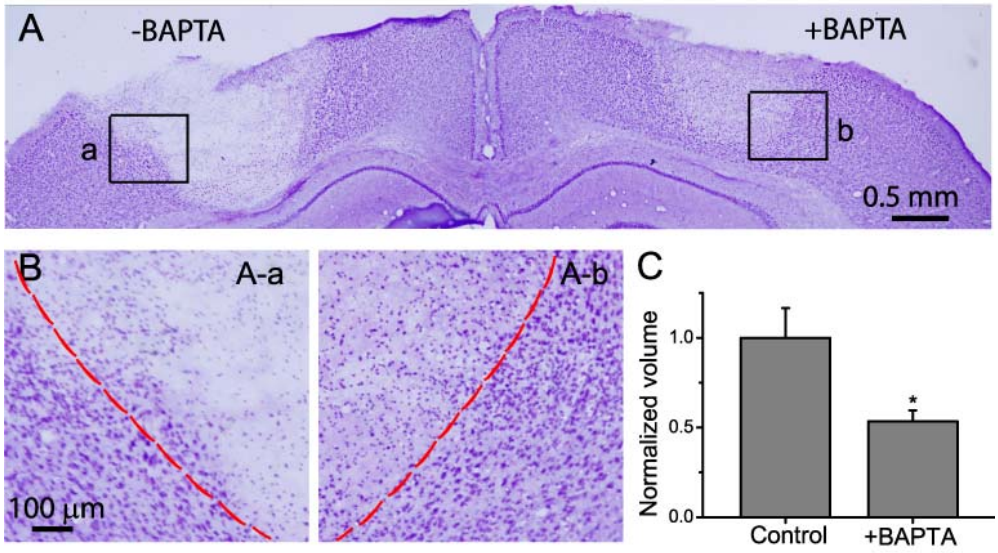

Figure 3.2. Effect of BAPTA-AM on photothrombosis-induced infarct volume. (**A**) Nissl staining of brain section. Photothrombosis was induced on both sides of barrel cortex region at the same time. An area of 1 mm diameter was illuminated in this experiment. (**B**) High resolution micrographs from the boxed areas in (**A**) showing distinct regions of ischemic cores and transition zones. (**C**) Normalized infarct volume indicated neuronal protective role of BAPTA-AM. Data were obtained from N=6 mice. * $p<0.05$, *t*-test.

3.3. Inhibition of calcium signal in cultured astrocytes using molecular biology

Although BAPTA can reduce bulk Ca^{2+} in astrocytes, Ca^{2+} signaling pathway targeted studies are required to gain insights into the mechanism of astrocyte Ca^{2+}-dependent neuronal damage after ischemia. Astrocytic Ca^{2+} signaling is largely due to the internal Ca^{2+} release after activation of the IP_3 receptor. Thus, disruption of the IP_3 signaling pathway might inhibit Ca^{2+} elevation after GPCR stimulation. The pleckstrin homology domain of PLC-like protein p130 (p130PH) efficiently binds IP_3, and consequently reduces receptor-stimulated Ca^{2+} elevation from internal stores (Lin et al., 2005; Várnai et al., 2002). Initially we tested whether the transient expression of p130PH in cultured astrocytes can inhibit ATP stimulated Ca^{2+} elevation. Our ultimate goal is to introduce this gene into astrocytes *in vivo* using viral transduction.

3.3.1. DNA plasmids containing transgene of IP_3 binding protein p130PH and reporter gene mRFP

Our lab originally obtained DNA plasmid pC1 - mRFP - p130PH (Figure 3.3) that contained a transgene mRFP-p130PH (a fusion protein) from Dr. György Hajnóczky (Thomas Jefferson University, Philadelphia, PA).

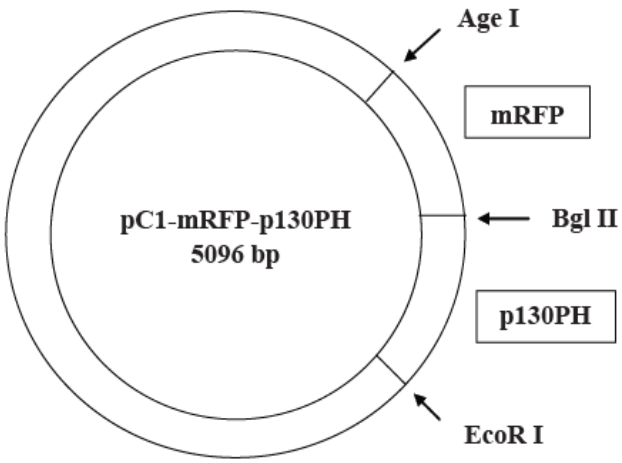

Figure 3.3. DNA plasmid pC1 - mRFP - p130PH for the positive experiment of Ca^{2+} signal imaging *in vitro*

Based on this plasmid, a new plasmid was constructed for the control experiments. In this new plasmid, I deleted the gene, which encodes mRFP - p130PH protein, with restriction enzymes Age I and EcoR I. Using a PCR method, we amplified DNA fragments mRFP with Age I at 5' end and EcoR I at 3' end using plasmid pC1-mRFP-p130PH as the template. Then, I ligated the inserts with pC1 plasmid to produce the new vector, which only contains the gene encoding protein mRFP. The constructed plasmid was digested with Age I and EcoR I restriction enzymes, and the result of agarose gel electrophoresis shows that two DNA bands were obtained: one is the plasmid pC1, with

the size of approximately 4.0 kb compared to the 1 kb DNA marker (the true size is 3971 bp); the other band is mRFP transgene, with the size in between of 1.0 kb and 0.5 kb (the true size is 698 bp). DNA sequencing was done afterward using DNA sequencing service proved by the DNA Core (University of Missouri) to confirm the correct insertion of the transgene. We named this new plasmid pC1 - mRFP (Figure 3.4).

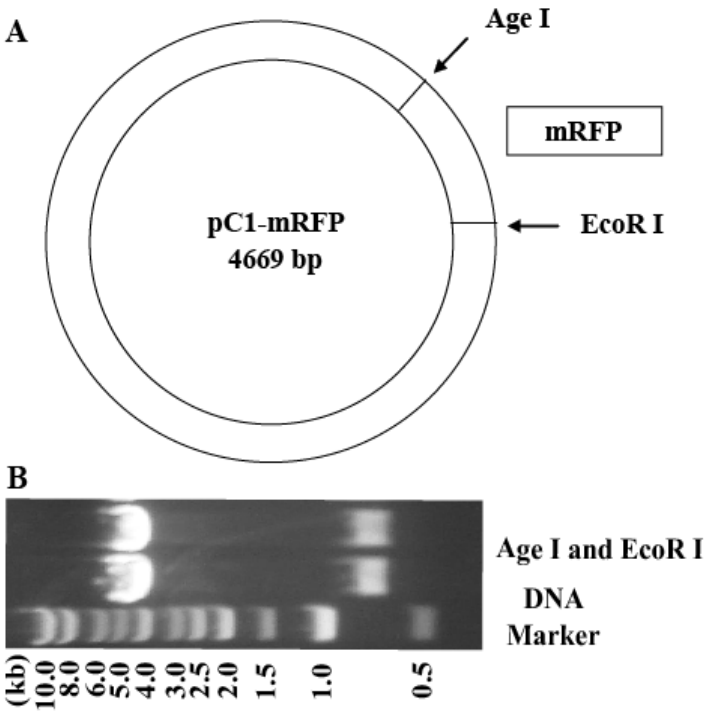

Figure 3.4. DNA plasmid pC1 – mRFP for the control experiment of Ca^{2+} signal imaging *in vitro*. (**A**) Map of pC1 - mRFP plasmid. (**B**) Agarose gel electrophoresis result of pC1 - mRFP digested with restriction enzymes Age I and EcoR I, mRFP fragment size: 698 bp.

3.3.2. Calcium imaging in cultured primary astrocytes

Initially, the *in vitro* experiments were conducted on primary cortical astrocytes (kindly provided by Dr. Grace Y. Sun's lab, Department of Biochemistry, University of Missouri) from newborn rat brains. I used plasmid pC1 – mRFP for the cell transfection as my control group. And for my positive group, I used plasmid pC1-mRFP-p130PH for

cell transfection. For the control experiments, 4 coverslips were prepared and 13 spots were chosen in total for Ca^{2+} imaging. Ca^{2+} imaging data was acquired from 495 cells, among which 69 cells were transfected (mRFP positive cells), while 426 cells were not transfected (mRFP negative cells). For the positive experiments, 6 coverlips were prepared and 6 spots were chosen in total for Ca^{2+} imaging. Ca^{2+} imaging data was acquired from 191 cells, and 27 of them were transfected (mRFP - p130PH positive cells), while 164 of them were not transfected (mRFP - p130PH negative cells).

While analyzing the data of Ca^{2+} signal, due to the overall performance of astrocytes, we noticed that not all of the astrocytes being used for the experiments were well functioned, thus we first calculated the Ca^{2+} signal response rate in both control and positive experiments. Using Metamorph software (Universal Imaging, CA), we carefully counted the total number of all the astrocytes imaged in these experiments as well as the number of cells that were with the expected Ca^{2+} signal response function: for non-transfected astrocytes, after being excited by 20 μM ATP, the Ca^{2+} concentration inside the cell increased and due to the flou-4 AM dye loading, an increase of fluorescent intensity was detected; for mRFP positive astrocytes, cells will show red fluorescence due to the mRFP transgene expression, however, since there's no p130PH protein expression, according to my hypothesis, there won't be any inhibition of Ca^{2+} release, thus, there should still be an increase of fluorescent intensity just as the non-transfected astrocytes; for mRFP-p130PH positive astrocytes, cells will show red fluorescence due to the mRFP transgene, moreover, due to the expression of p130PH protein, according to my hypothesis, the release of Ca^{2+} inside the cell will be inhibited, thus, the fluorescent intensity should stay the same throughout the time course. (some slight decrease may

occur due to photobleaching). The Ca^{2+} signal response rate was defined as the number of cells with fluorescent intensity increased divided by the total cell number. Results are summarized in Tables 3.1 and 3.2 below, which demonstrates that in cultured primary astrocytes, the control experiments show a response rate of 86.9% for mRFP negative cells, and 75.4% for mRFP positive cells. As for the positive experiments, the response rate of mRFP – p130PH negative cells was 91.5%; 29.6% for mRFP – p130PH positive cells. These statistical analyses indicated that a majority of cells exhibited the expected Ca^{2+} signal response. Hence, these data are shown to be statistically reliable.

Table 3.1. Summary of the Ca^{2+} signal response rate in cultured primary astrocytes from the control experiments

Cell number	Non-transfected (mRFP negative)	mRFP positive
Total cell	426	69
Cells with fluorescent intensity increase	370	52
Response rate (%)	86.9	75.4

Table 3.2. Summary of the Ca^{2+} signal response rate in cultured primary astrocytes from the positive experiments

Cell number	Non- transfected (mRFP – p130PH negative)	mRFP - p130PH positive
Total cell	164	27
Cells with fluorescent intensity increase	150	8
Response rate (%)	91.5	29.6

Data were analyzed using the Metamorph software (Universal Imaging, CA) to generate background-subtracted $\Delta F/Fo$ time courses, where Fo was resting fluorescence and ΔF was the change in florescence from the resting value. Histograms (Figure 3.5 D

and Figure 3.6 D) and trace of time course (Figure 3.5 C and Figure 3.6 C) were generated using Excel (Micro Software, CA) for both control and positive experiments in cultured primary astrocytes.

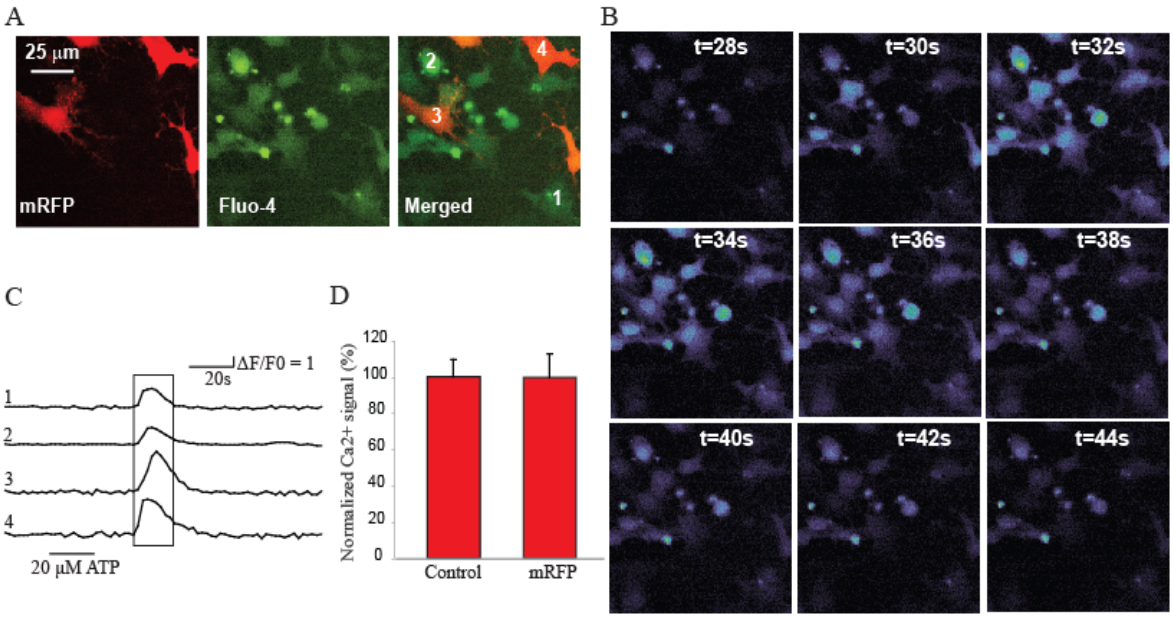

Figure 3.5. Cultured primary astrocytes exhibit enhanced Ca^{2+} signals in response to ATP stimulation. (**A**) Cultured primary astrocytes labeled with fluo-4 after transfected by DNA plasmid pC1 – mRFP. (**B**) Representative images of Ca^{2+} responses in astrocytes loaded with fluo-4. (**C**) Time course of Ca^{2+} elevations expressed as $\Delta F/F_0$ in astrocytes with (cells 3 and 4) and without (cells 1 and 2) expression of pC1 – mRFP. 20 μM ATP was applied from 20 s to 40 s. The number of the traces corresponds to the cells in merged image in (**A**) as indicated. The box region corresponds to the images in (**B**) as indicated. All cells were recorded in the same image frame. (**D**) Summary of astrocytic Ca^{2+} signals expressed as a peak value of $\Delta F/F_0$. The data were collected from cultured primary astrocytes N=16 cells for the non-transfected control group (mRFP negative) and N=9 cells for the transfected group (mRFP positive). Statistical analyses between mRFP negative group and mRFP positive group were assessed using *t*-test. $P>0.05$

For the control experiments, cells showing red fluorescence indicated astrocytes with protein mRFP expressed inside the cells. Incubation of fluo-4 AM led to the labeling of fluo-4 into astrocytes (Figure 3.5 A). Both transfected (mRFP positive) and non-transfected (mRFP negative) astrocytes exhibited enhanced Ca^{2+} signals after 20 μM ATP excitation (Figure 3.5 C). The summary data show the percentage of normalized Ca^{2+} fluorescent intensity peak value (Figure 3.5 D), and *t*-test analysis shows that data from

mRFP negative cells and mRFP positive cells with a *P* value larger than 0.05 means there is no significant difference between these two groups. We concluded that the control experiments on cultured primary astrocytes proved that mRFP protein does not affect the Ca^{2+} signal in astrocytes. Thus, it is safe to be used as a marker to identify transfected cells (mRFP - p130PH positive cells).

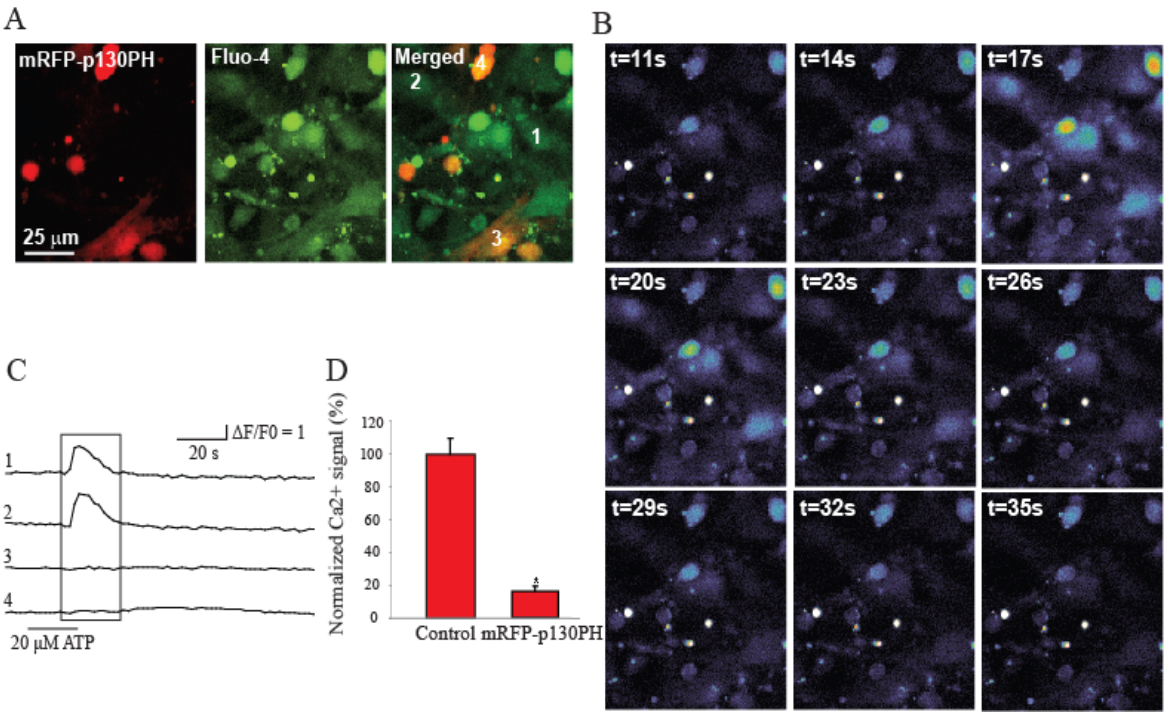

Figure 3.6. Inhibition of Ca^{2+} signals by p130PH in cultured primary astrocytes. (**A**) Cultured primary astrocytes astrocytes labeled with fluo-4 after transfected by DNA plasmid pC1 – mRFP – p130PH. (**B**) Representative images of Ca^{2+} responses in astrocytes loaded with fluo-4. (**C**) Time course of Ca^{2+} oscillations expressed as $\Delta F/F_0$ in astrocytes with (cells 3 and 4) and without (cells 1 and 2) expression of pC1 – mRFP – p130PH. 20 μM ATP was applied from 20 s to 40 s. The number of the traces corresponds to the cells in merged image in (**A**) as indicated. The box region corresponds to the images in (**B**) as indicated. All cells were recorded in the same image frame. (**D**) Summary of astrocytic Ca^{2+} signals expressed as a peak value of $\Delta F/F_0$. The data were collected from cultured primary astrocytes N=16 cells for the non-transfected control group (mRFP – p130PH negative) and N=9 cells for the transfected group (mRFP – p130PH positive). Statistical analyses between mRFP – p130PH negative group and mRFP – p130PH positive group were assessed using *t*-test. **P*>0.05

For the positive experiments, astrocytes expressing protein mRFP - p130PH were identified by red fluorescence. For Ca^{2+} imaging, astrocytes were labeled with fluo-4 (Figure 3.6 A). When stimulated with 20 μM ATP, only non-transfected (mRFP – p130PH negative) astrocytes exhibited Ca^{2+} elevations (Figure 3.6 C, trace 1 and 2). However, transfected (mRFP – p130PH positive) astrocytes exhibited flat Ca^{2+} signal traces throughout the time course (Figure 3.6 C, trace 3 and 4). Also, from the summary data (Figure 3.6 D), the percentage of normalized Ca^{2+} fluorescent intensity peak value from mRFP – p130PH positive astrocytes was reduced by approximately 85% as compared to those non-transfected astrocytes (mRFP – p130PH negative). *t*-test analysis of these two groups showed a *P* less than 0.05, which indicated a statistically significant difference between these two groups. Thus, we concluded that protein p130PH expressed in astrocytes can significantly inhibit ATP stimulated Ca^{2+} elevations.

3.3.3. Calcium imaging in a cell line of astrocytes

After both control and positive experiments were conducted on cultured primary astrocytes, we would like to confirm whether p130PH can also inhibit ATP-induced Ca^{2+} signals in a cell line of astrocyte (DITNC cells, ATCC CRL-2005). Thus, we applied the same experimental protocol on cultured DITNC cells.

We were using the same plasmid pC1-mRFP for the cell transfection in the control group. For the positive group, we used plasmid pC1-mRFP-p130PH for cell transfection. For the control experiments, 4 coverslips were prepared and 2 spots were chosen for each coverslip for Ca^{2+} imaging (8 spots in total). Ca^{2+} imaging data was acquired from 242 cells, among which 73 cells were transfected (mRFP positive cells), while 163 cells were

not transfected (mRFP negative cells). For the positive experiments, 4 coverslips were prepared and for each coverslip 2 spots were chosen for Ca^{2+} imaging (8 spots in total). Ca^{2+} imaging data was acquired from 259 cells, and 66 of them were tramsfected (mRFP - p130PH positive cells), while 193 of them were not transfected (mRFP - p130PH negative cells).

Just as with the cultured primary astrocytes experiments, the Ca^{2+} signal response rate in both control and positive experiments were calculated first. Using Metamorph software (Universal Imaging, CA), The total number of all the astrocytes being used in these experiments, as well as the number of cells that were with the expected Ca^{2+} signal response function (expected Ca^{2+} signal response function was carefully described earlier in Chapter 3.3.2.) were carefully counted. Also the Ca^{2+} signal response rate meant the number of cells with fluorescent intensity increase divided by the total cell number, results are summarized in Tables 3.3 and 3.4 below, which tells us that in the cultured astrocytes cell line, the control experiments showed a response rate of 80.5% for mRFP negative cells, and 74.0% for mRFP positive cells. As for the positive experiments, the response rate of mRFP – p130PH negative cells was 75.7%, and 4.6% for mRFP-p130PH positive cells. These statistical analyses are reasonable and indicated that a majority of cells exhibited the expected Ca^{2+} signal response. Hence, these data are shown to be statistically reliable.

Table 3.3. Summary of the Ca^{2+} signal response rate in cultured astrocytes cell line from the control experiments

Cell number	Non-transfected (mRFP negative)	mRFP positive
Total cell	169	73
Cells with fluorescent intensity increase	136	54
Response rate (%)	80.5	74.0

Table 3.4. Summary of the Ca^{2+} signal response rate in cultured astrocytes cell line from the positive experiments

Cell number	Non-transfected (mRFP-p130PH negative)	mRFP-p130PH positive
Total cell	193	66
Cells with fluorescent intensity increase	146	3
Response rate (%)	75.7	4.6

Furthermore, data were analyzed using the Metamorph software (Universal Imaging, CA), Origin software (OriginLab Corporation, MA) and Excel (Micro Software, CA) for both control and positive experiments in the cultured astrocytes cell line as described in Chapter 3.3.2.

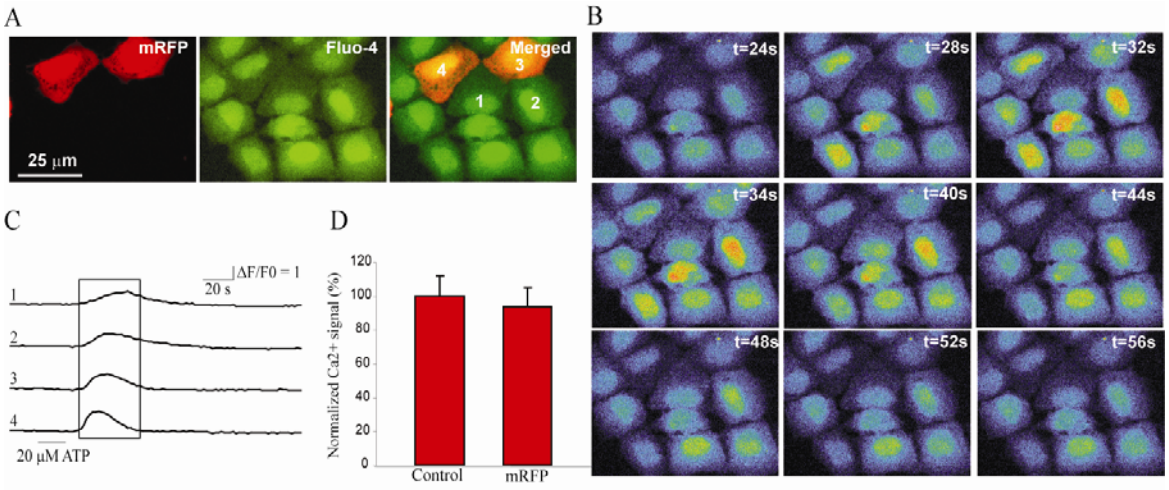

Figure 3.7. Cultured astrocytes cell line exhibit enhanced Ca^{2+} signals in response to ATP stimulation. (**A**) Cultured astrocytes cell line labeled with fluo-4 after transfected by DNA plasmid pC1 – mRFP. (**B**) Representative images of Ca^{2+} responses in astrocytes loaded with fluo-4. (**C**) Time course of Ca^{2+} elevations expressed as $\Delta F/F_0$ in astrocytes with (cell 3 and 4) and without (cell 1 and 2) expression of pC1 – mRFP. 20 μM ATP was applied from 20 s to 40 s. The number of the traces corresponds to the cells in merged image in (**A**) as indicated. The box region corresponds to the images in (**B**) as indicated. All cells were recorded in the same image frame. (**D**) Summary of astrocytic Ca^{2+} signals expressed as a peak value of $\Delta F/F_0$. The data were collected from cultured astrocytes cell line N=24 cells for the non-transfected control group (mRFP negative) and N=26 cells for the transfected group (mRFP positive). Statistical analyses between mRFP negative group and mRFP positive group were assessed using *t*-test. $P>0.05$

For the control experiments, cells showing red fluorescence indicated astrocytes with protein mRFP successfully expressed inside the cells. Incubation of fluo-4 AM led to labeling of fluo-4 into astrocytes (Figure 3.7 A). Both transfected (mRFP positive) and non-transfected (mRFP negative) astrocytes exhibited enhanced Ca^{2+} signals after 20 μM ATP excitation (Figure 3.7 C). The histograms show the normalized percentage of Ca^{2+} fluorescent intensity peak value (Figure 3.7 D), and *t*-test analysis shows that data from mRFP negative cells and mRFP positive group with a P larger than 0.05, which means there is no significant difference between these two groups. Thus, we concluded that the control experiments on a cultured astrocyte cell line showed the same performance as cultured primary astrocytes, which also proved that mRFP protein does not affect the

Ca^{2+} signal in astrocytes. Thus, it is safe to be used as a marker to identify transfected cells.

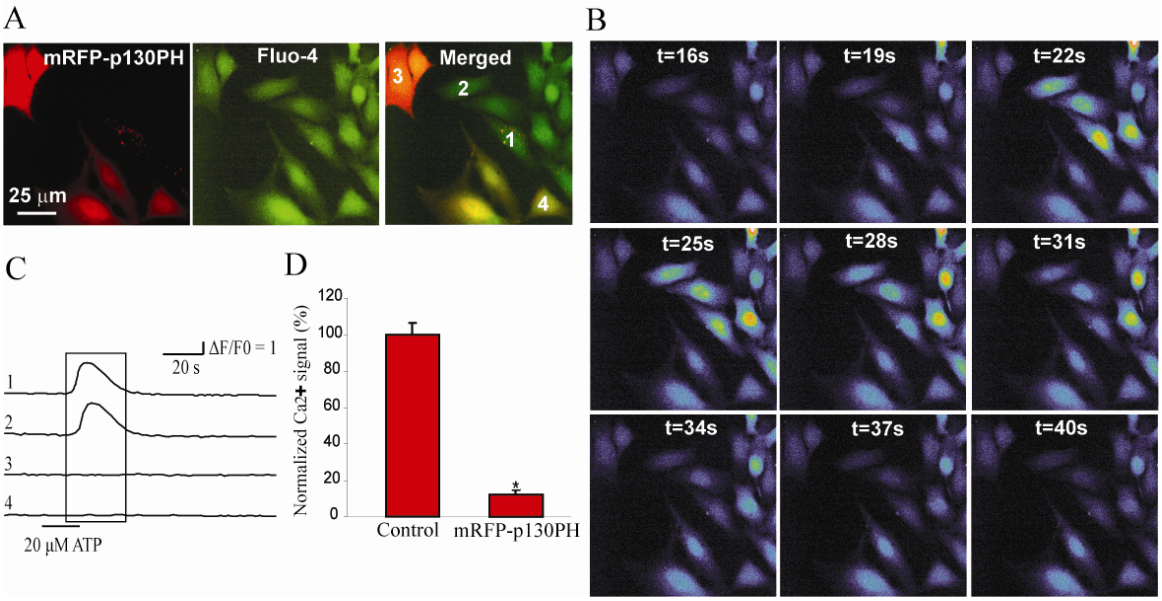

Figure 3.8. Inhibition of Ca^{2+} signals by p130PH in cultured astrocytes cell line. (**A**) Cultured astrocytes cell lines labeled with fluo-4 after transfected by DNA plasmid pC1 – mRFP – p130PH. (**B**) Representative images of Ca^{2+} responses in astrocytes loaded with fluo-4. (**C**) Time course of Ca^{2+} oscillations expressed as $\Delta F/F_0$ in astrocytes with (cell 3 and 4) and without (cell 1 and 2) expression of pC1 – mRFP – p130PH. 20 μM ATP was applied from 20 s to 40 s. The number of the traces corresponds to the cells in merged image in (**A**) as indicated. The box region corresponds to the images in (**B**) as indicated. All cells were recorded in the same image frame. (**D**) Summary of astrocytic Ca^{2+} signals expressed as a peak value of $\Delta F/F_0$. The data were collected from cultured astrocytes cell line N=38 cells for the non-transfected control group (mRFP – p130PH negative) and N=34 cells for the transfected group (mRFP – p130PH positive). Statistical analyses between mRFP – p130PH negative group and mRFP – p130PH positive group were assessed using *t*-test. **P*<0.05

For the positive experiments, astrocytes expressing protein mRFP-p130PH can be identified by red fluorescence. For Ca^{2+}, astrocytes were labeled with fluo-4 (Figure 3.8 A). When stimulated with 20 μM ATP, only non-trasfected (mRFP – p130PH negative) astrocytes exhibited Ca^{2+} elevations (Figure 3.8 C, trace 1 and 2). However, transfected (mRFP – p130PH positive) astrocytes exhibited flat Ca^{2+} signal traces throughout the time courses (Figure 3.8 C, trace 3 and 4). Also, from the histograms (Figure 3.8 D), the

percentage of normalized Ca^{2+} fluorescent intensity peak value from mRFP – p130PH positive astrocytes was reduced by about 90% compared to non-transfected astrocytes (mRFP – p130PH negative astrocytes). *t*-test analysis of these two groups shows a *P* value less than 0.05, which indicates significant differences between these two groups. Thus, the positive experiments on a cell line of astrocyte showed the same response as cultured primary astrocytes. Together, these data confirm that protein p130PH expressed in astrocytes can significantly inhibit ATP stimulated Ca^{2+} elevations.

3.4. Construction of transgene expressing plasmids of recombinant adeno-associated virus (rAAV) vectors with astrocyte specific GFAP promoter ABC1D

Results obtained from cultured primary astrocytes as well as an astrocytic cell line demonstrate that mRFP-p130PH expressed in astrocytes can significantly inhibit ATP-induced Ca^{2+} signal. Expression of reporter protein mRFP does not affect the Ca^{2+} signal in astrocytes. Our goal was to selectively express mRFP-p130PH in astrocytes *in vivo* and to test whether p130PH has neuronal protective effect after ischemia.

Currently, there are two approaches to introduce transgenes *in vivo*. The first is to generate transgenic mice. But generation of transgenic mice is expensive and time consuming. In addition, transgene might be lethal or cause developmental defects in mice. Viral transduction provides an alternative approach to locally introduce transgene into different brain regions. This approach is increasingly used to introduce foreign genes into the nervous system because many types of virus can deliver genes to the non-dividing cells including brain neurons (Davidson and Breakefield, 2003). It provides a flexible approach for regional gene delivery. Furthermore, using a cell type-specific promoter, it

is feasible to selectively deliver transgene to a specific type of cells *in vivo*. In this study, we attempted to use recombinant adeno-associated virus (rAAV) to introduce the pleckstrin homology (PH) domain of PLC-like protein p130 (p130PH) into astrocytes to disrupt the Ca^{2+} signaling pathway. rAAV vectors were chosen because they are highly effective for gene delivery, non-pathogenic and can express a transferred gene for the life of the animal (Cearley and Wolfe, 2006). Our lab originally obtained AAV cis - plasmid pZac2.1-CMV (cloning vector) from the Vector Core at University of Pennsylvania. It contains two AAV2 inverted terminal repeats (ITRs) at the two ends, the CMV promoter, the multiple cloning sites (MCS) and SV40 poly A for easy cloning for the gene of interest. Based on this plasmid, we constructed new vectors both for the control and positive experiments *in vivo*.

3.4.1. rAAV virus plasmid with GFAP promoter ABC1D: pZac2.1 – ABC1D

To achieve astrocyte-specific expression of transgene, we inserted a recently generated glial fibrillary acidic protein (GFAP) promoter, gfaABC1D (Lee et al., 2008), into a *cis* cloning plasmid. The GFAP promoter ABC1D was provided by Dr. Michael Brenner (University of Alabama-Birmingham).

As a first step, we swamped CMV promoter in plasmid pZac2.1-CMV with GFAP promoter. We ligated this GFAP promoter into AAV cis - plasmid pZac2.1-CMV using restriction enzymes Bgl II and EcoR I. The constructed vector was then digested with Bgl II, EcoR I and Sma I restriction enzymes, and the result of agarose gel electrophoresis showed that two DNA bands were obtained after Bgl II and EcoR I digestion: one is the rAAV virus plasmid pZac2.1, with the size of approximately 4.0 kb compared to the 1 kb

DNA marker (the true size is 3474 bp); the other band is transgene GFAP promoter ABC1D, with the size approximately 0.75 kb (the true size is 717 bp). According to the DNA sequence of plasmid pZac2.1 – ABC1D, there are 6 Sma I sites (located at 289, 300, 1026, 1189, 1585, 1596), therefore, after the Sma I complete digestion, theoretically, there should be 6 DNA fragments with the size of 12 bp, 727 bp, 164 bp, 397 bp, 12 bp and 2882 bp, respectively. From the result of agarose gel electrophoresis, four DNA bands were obtained: one with the size approximately 3.0 kb (2882 bp), with one between 1.0 kb and 0.5 kb (727 bp), and the other two less than 0.5 kb (397 bp and 164 bp). These results were reasonable and considered to be correct, since size 12 bp is too small to be detected by DNA agarose gel electrophoresis; the other four bands that were noticeable on the agarose gel were with correct sizes. The plasmid was sequenced in the DNA Core (University of Missouri) to confirm the correct insertions of the promoter. This plasmid was named as pZac2.1 – ABC1D (Figure 3.9), and will be used for other new plasmid construction in the next steps.

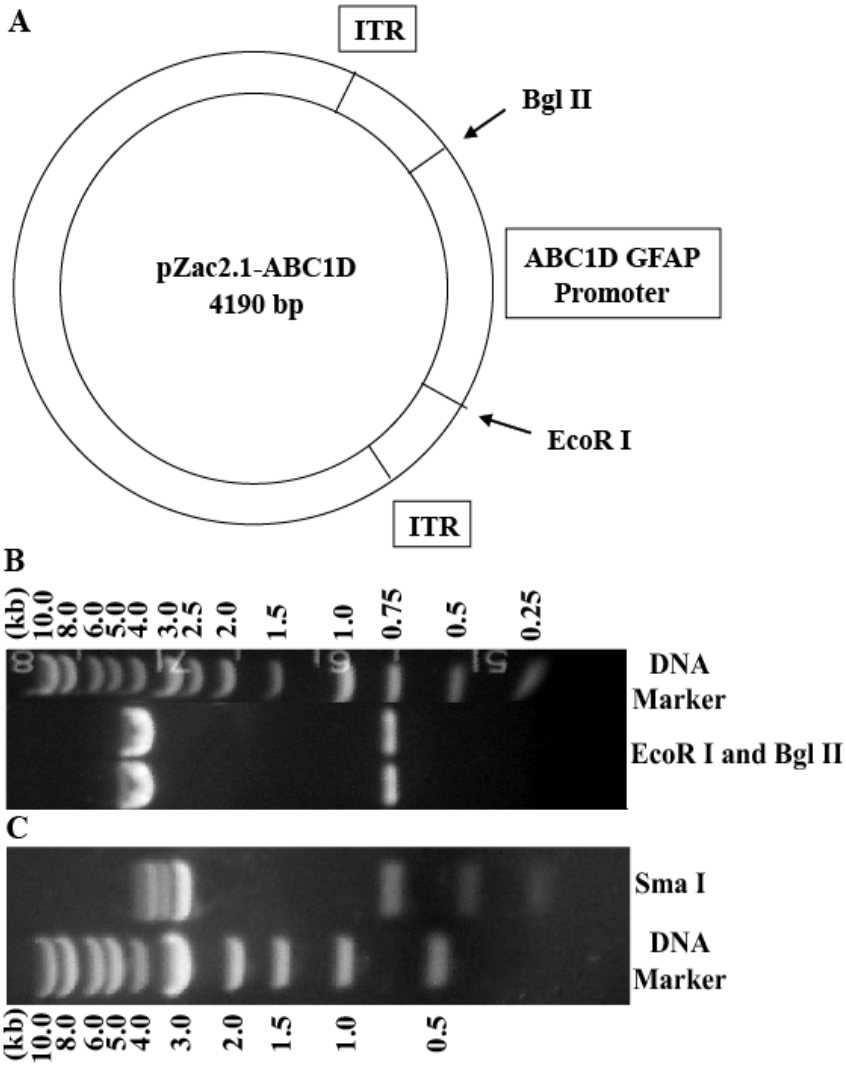

Figure 3.9. Construction of DNA plasmid pZac2.1-ABC1D for rAAV vector. (**A**) Map of pZac2.1 - ABC1D plasmid. (**B**) Agarose gel electrophoresis result of pZac2.1 - ABC1D plasmid digested with restriction enzymes EcoR I and Bgl II, ABC1D GFAP promoter fragment size: 717 bp. (**C**) Agarose gel electrophoresis result of pZac2.1 - ABC1D plasmid digested with restriction enzyme Sma I.

3.4.2. Construction of viral plasmid pZac2.1-ABC1D-mRFP for control experiments

Our next step is to insert the transgene p130PH and reporter gene mRFP into the pZac2.1-ABC1D plasmid. Using the original plasmid pC1 - mRFP - p130PH as a template, we generated a PCR fragment mRFP with EcoR I site at both 3' and 5' end.

Then we inserted this transgene into a previously constructed virus plasmid pZac2.1-ABC1D. The new plasmid was then test digested with EcoR I and Sma I restriction enzymes. The result of agarose gel electrophoresis shows that two DNA bands were obtained after EcoR I digestion: one is the rAAV virus plasmid pZac2.1-ABC1D, with the size of approximately 4.0 kb compared to the 1 kb DNA marker (the true size is 4190 bp); the other band is the transgene mRFP with the size between 1.0 kb and 0.5 kb (the true size is 698 bp). According to the DNA sequence of plasmid pZac2.1-ABC1D-mRFP, there are 6 Sma I sites (located at 289, 300, 1026, 1887, 2283, 2294); therefore, after Sma I complete digestion, theoretically, there should be 6 DNA fragments with the size of 12 bp, 727 bp, 862 bp, 397 bp, 12 bp and 2882 bp, respectively. From the result of agarose gel electrophoresis, four DNA bands were obtained: one with the size around 3.0 kb (2882 bp), two with the size a little less than 1.0 kb (727 bp and 862 bp), and the other one less than 0.5 kb (397 bp). These results are reasonable and considered to be correct, since size 12 bp is too small to be detected by DNA agarose gel electrophoresis; the other four bands that are noticeable on the agarose gel are with correct sizes. The plasmid was sequenced in the DNA Core (University of Missouri) to confirm the correct insertions of promoter and transgene. This plasmid was named as pZac2.1 - ABC1D - mRFP (Figure 3.10), and will be used for our control experiments *in vivo*.

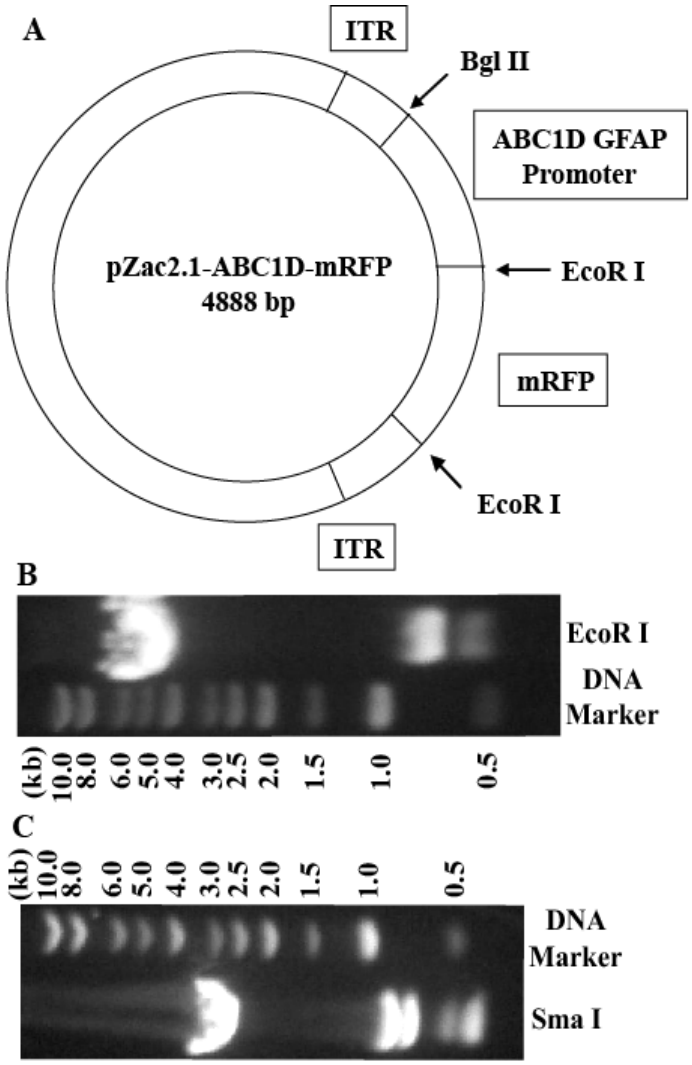

Figure 3.10. Construction of DNA plasmid pZac2.1- ABC1D - mRFP for the control experiment *in vivo.* (**A**) Map of pZac2.1 - ABC1D - mRFP plasmid. (**B**) Agarose gel electrophoresis result of pZac2.1 - ABC1D - mRFP plasmid digested with restriction enzyme EcoR I, mRFP fragment size: 698 bp. (**C**) Agarose gel electrophoresis result of pZac2.1 - ABC1D - mRFP plasmid digested with restriction enzyme Sma I.

3.4.3 Construction of viral plasmid pZac2.1 – ABC1D – mRFP – p130PH for positive experiments

Using the same strategy, we constructed another rAAV virus plasmid that contains p130PH, namely, pZac2.1 – ABC1D – mRFP – p130PH, for our positive experiments.

Using plasmid pC1 - mRFP - p130PH as a template, we generated PCR fragment mRFP – p130PH with EcoR I site at both 3' and 5' end. Then we inserted this transgene into a previously constructed virus plasmid pZac2.1 - ABC1D. The constructed vector was then test digested with EcoR I and Sma I restriction enzymes. The result of agarose gel electrophoresis shows that two DNA bands were obtained after EcoR I digestion: one is the rAAV virus plasmid pZac2.1 - ABC1D, with the size of approximately 4.0 kb compared to the 1 kb DNA marker (the true size is 4190 bp); the other band is the transgene mRFP – p130PH, with the size of approximately 1.0 kb compared to the 1 kb DNA marker (the true size is 1125 bp). According to the DNA sequence of plasmid pZac2.1 - ABC1D - mRFP - p130PH, there are 6 Sma I sites (located at 289, 300, 1026, 2314, 2710, 2721); therefore, after Sma I complete digestion, theoretically, there should be 6 DNA fragments with the size of 12 bp, 727 bp, 1289 bp, 397 bp, 12 bp and 2882 bp, respectively. From the results of agarose gel electrophoresis, four DNA bands were obtained: one with the size approximately 3.0 kb (2882 bp), one approximately 1.5 kb to 1.0 kb (1289 bp), one with the size a little less than 1.0 kb (727 bp), and one less than 0.5 kb (397 bp). These results are reasonable and considered to be correct, since size 12 bp is too small to be detected by DNA agarose gel electrophoresis; the other four bands that are noticeable on the agarose gel are correct sizes. The plasmid was sequenced in DNA Core (University of Missouri) to confirm the correct insertions of the promoter and transgene. This plasmid was named pZac2.1 - ABC1D – mRFP – p130PH (Figure 3.11), and will be used for the positive experiments *in vivo*.

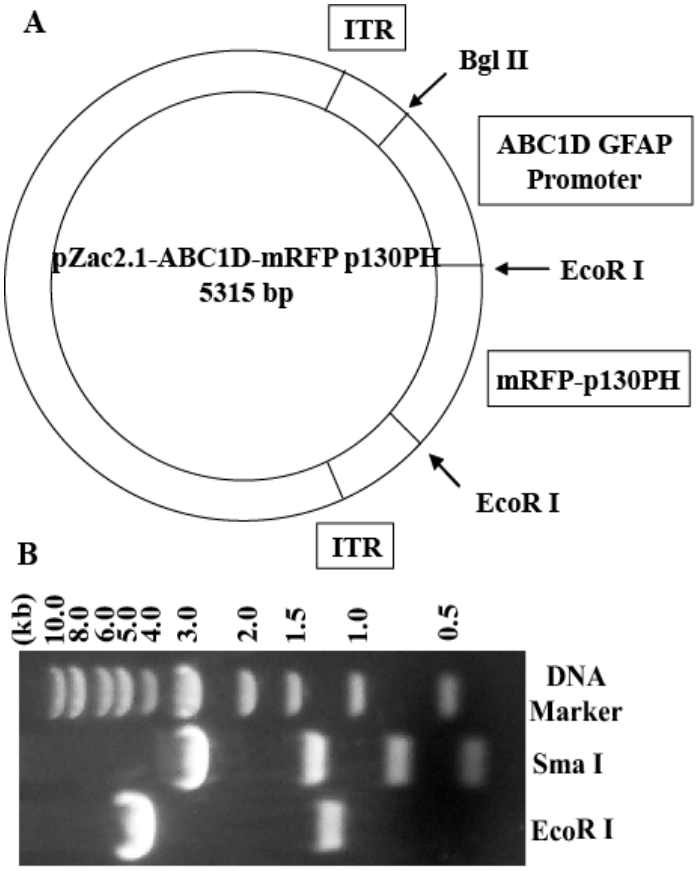

Figure 3.11. Constructions of DNA plasmid pZac2.1 - ABC1D - mRFP - p130PH for the positve experiment *in vivo*. (**A**) Map of pZac2.1 - ABC1D - mRFP - p130PH plasmid. (**B**) Agarose gel electrophoresis result of pZac2.1 - ABC1D - mRFP - p130PH plasmid digested with restriction enzymes EcoR I and Sma I, mRFP - p130PH fragment size: 1125 bp

3.5. Selective expression of mRFP-p130PH in astrocytes in the cortex of mouse brain by rAAV vector transduction

Pseudo-type 2/5 rAAV (rAAV2/5) vectors with serotype 2 AAV (AAV2) *rep* and serotype 5 AAV (AAV5) *cap* gene were chosen because this serotype has been suggested to have tropism for astrocytes (Tenenbaum et al., 2004; Davidson et al., 2000). rAAV vectors were produced by triple transfection of H293 at the University of Pennsylvania Gene Therapy Program Vector Core and have a titer of 8×10^{12} genomic copies (GC) per

ml. Briefly, this *cis* plasmid was cotransfected with an AAV *trans* plasmid (AAV2/5) encoding serotype 2 AAV (AAV2) *rep* and serotype 5 AAV (AAV5) *cap* genes and an adenoviral helper plasmid in HEK 293 cells to produce pseudo-type rAAV2/5 vectors. The vectors were purified using a method based on buoyant density (Cesium chloride) ultracentrifugation and collected in 5% glycerol in PBS (Fisher et al., 1997). Plasmids were stored in aliquots at -80 °C and thawed on ice before use. The vectors were injected into the cortex of mouse brain to deliver p130PH to astrocytes. p130PH expression profiles were assessed at two weeks after injection by directly visualizing the fluorescence of fusion protein in the brain sections.

3.5.1. rAAV-mediated transgene expression in the cortex

Two weeks after microinjection with viral vectors pZac2.1-ABC1D-mRFP-p130PH into the cortex of mouse brain, mice were sacrificed and transcardially perfused for histological study. We were able to localize the rAAV2/5 transduced cortical region in the whole brain after fixation with PFA by epi-fluorescence microscopy, indicating the expression of the fusion protein mRFP (Figure 3.12). Confocal microscopy was used to directly visualize the individual mRFP-p130PH expressing cells in coronal brain sections. The mRFP-p130PH expressing cells had a bushy morphology with many fine terminal processes from the primary processes (Figure 3.12 D) which resemble astrocytes using *in vivo* imaging (Ding et al., 2007; Nimmerjahn et al., 2004; Wilhelmsson et al., 2006), suggesting specific expression of transgene mRFP-p130PH in astrocytes driven by gfaABC$_1$D promoter. rAAV2/5 transduction resulted in broad distribution of mRFP-positive cells throughout all cortical layers. Normally a region of 600-800 μm can be

identified. Thus, the data indicate that transgene mRFP-p130PH was selectively expressed in astrocytes in the cortex with viral transduction.

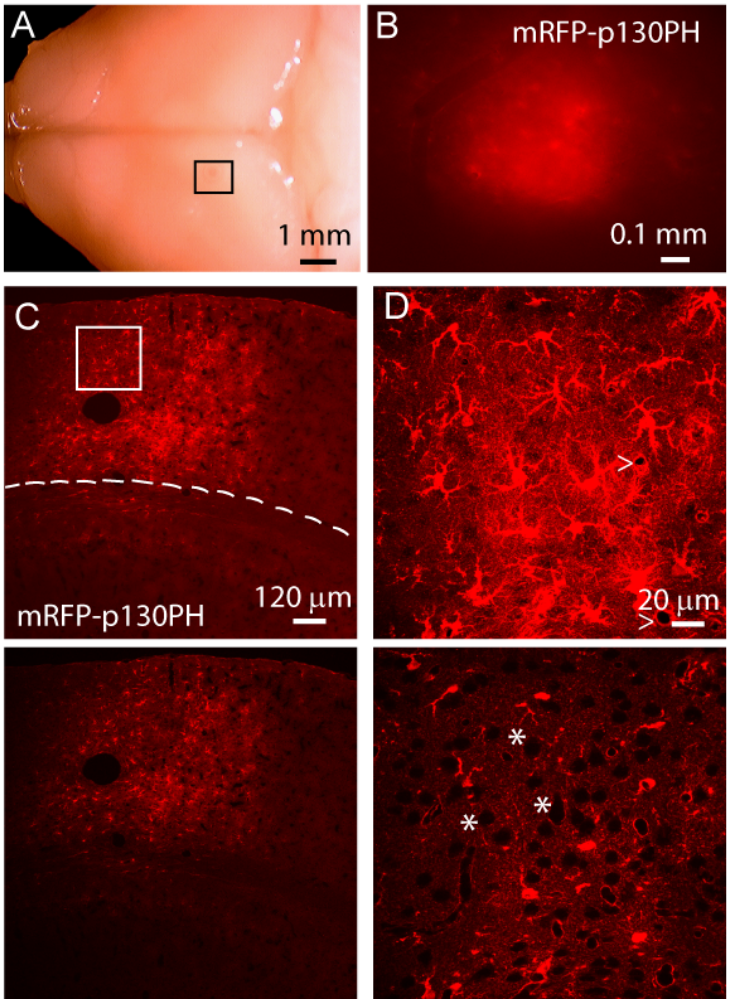

Figure 3.12. Expression of transgene mRFP-p130PH *in vivo* by rAAV transduction. (**A**) A PFA fixed whole mouse brain indication the injection site in boxed region. (**B**) Micrographs with low resolution from epi-fluorescence imaging showing the expression of mRFP fluorescence in the injected region from (**A**). (**C**)- (**D**) Confocal images of mRFP-p130PH positive cells in the injected region in a coronal section of the cortex with different resolutions. (**D**) is the image from the boxed region of (**C**). The upper panels were images of maximal projection, and the lower panels were images of single optical section from the upper panel.

3.5.2. Specific expression of mRFP-p130PH in astrocytes by viral transduction

Although we expected the transduced cells were astrocytes because we used an astrocyte specific promoter, we further stained brain sections with an antibody against an

astrocyte-specific marker, GFAP, to confirm whether mRFP-p130PH is selectively expressed in astrocytes. Figure 3.13 A-C shows a transduced section with different resolutions stained with GFAP antibody. Notably, astrocytes were expressed with GFAP in the dorsal surface of cortex in transduced region (Figure 3.13 A and B), these cells were colocalized with mRFP, however, only a slender expression of GFAP was observed in the deep layers of cortex where many cells were transduced and can be identified by mRFP fluorescence (Figure 3.13 A and C). Our results show that the majority of GFAP positive astrocytes expressed mRFP in the regions (n=7 sections from 4 mice, 164 GFAP positive cells and 155 mRFP positive cells), demonstrating the high efficiency of viral transduction for astrocyte-specific expression of transgene driven by gfaABC1D promoter.

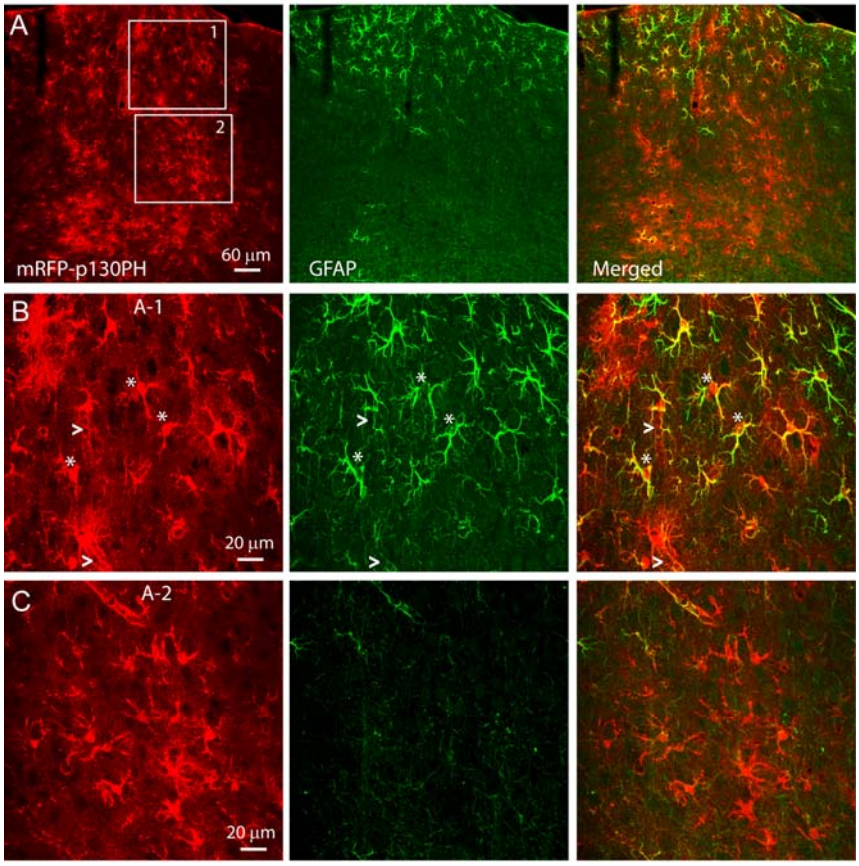

Figure 3.13. Selective expression of transgene mRFP-p130PH in astrocytes in the cortex. (**A**) Confocal images of mRFP fluorescence (left) and astrocyte markers GFAP (middle) staining of low resolution. (**B**)-(**C**) Confocal images of mRFP fluorescence (left) and astrocyte markers GFAP (middle) staining of high resolution. Both (**A**) and (**B**) are maximal projection images and (**C**) is single optical section image.

We also stained the transduced brain sections with antibodies against NeuN and Iba1, specific protein markers for neurons and microglia. In whole transduced region including the deep layers of the cortex, no co-localization between mRFP fluorescence and NeuN signal was observed (Figure 3.14). Notably, although there was overlap between mRFP fluorescence and NeuN signal in maximal projection images due to 3-D nature (Figure 3.14 B), they were not colocalized. This can be confirmed from the single optical section images from the same brain section, where neurons were surrounded by mFRP

fluorescence (Figure 3.14 C) and not a single mFRP-expressing cell was colocalized with NeuN signal.

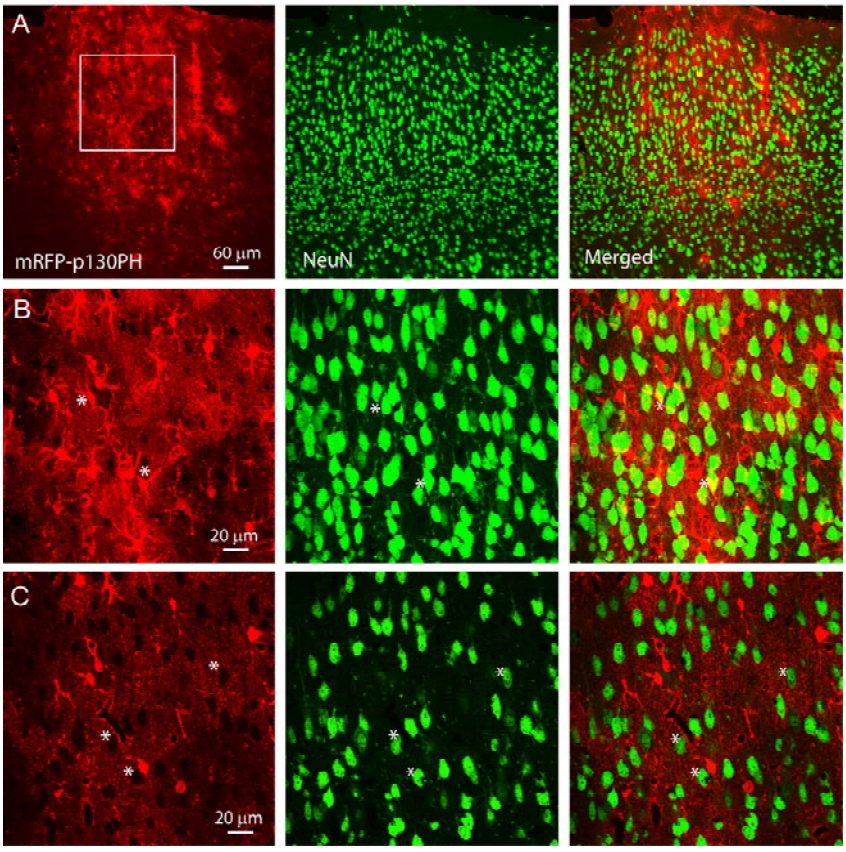

Figure 3.14. The transgene mRFP-p130PH was not expressed in neurons. (**A**) Confocal images of mRFP fluorescence (left) and neuron markers NeuN (middle) staining of low resolution. (**B**)-(**C**) Confocal images of mRFP fluorescence (left) and neuron markers NeuN (middle) staining of high resolution. Both (**A**) and (**B**) are maximal projection images and (**C**) is single optical section image.

Similarly, Iba1 signal was not colocalized with mRFP fluorescence (Figure 3.15). Thus we concluded that p130PH-mRFP is exclusively expressed in astrocytes driven by gfaABC1D promoter in the brain mediated by viral transduction.

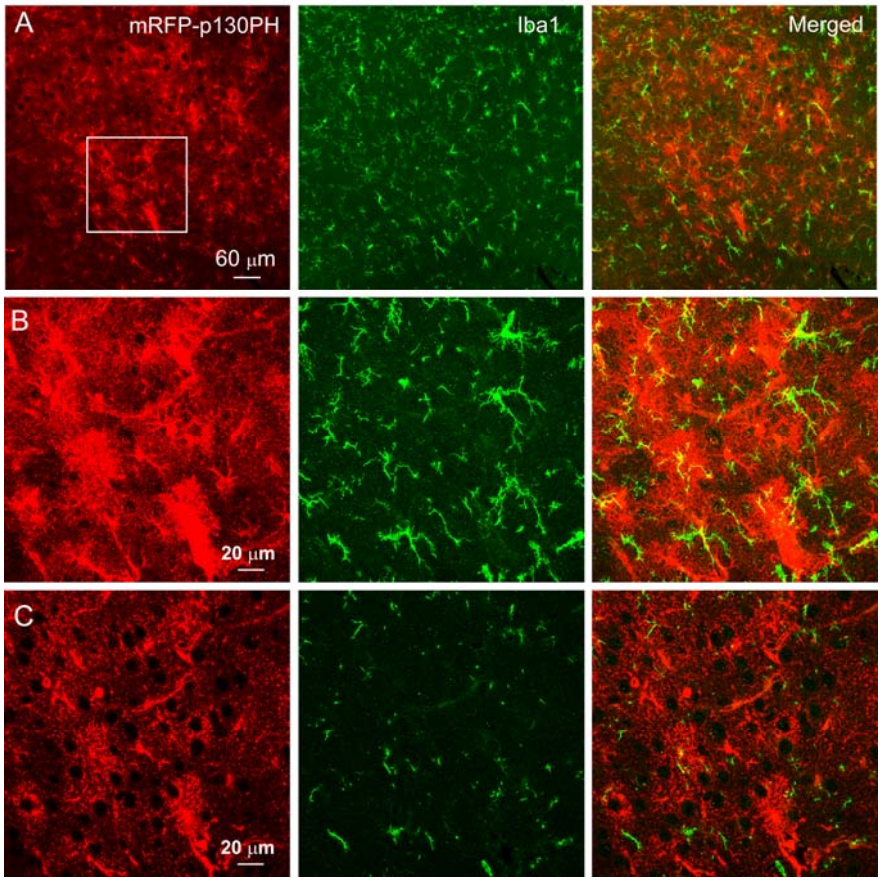

Fig 3.15: The transgene mRFP-p130PH fluorescence was not expressed in microglia. (**A**) Maximal projection images of mRFP-p130PH fluorescence and Iba1 signal in transduced region in the cortex. (**B**) High resolution maximal projection images of mRFP-p130PH fluorescence and Iba1 signal from the boxed region in (**A**). (**C**) Single optical sections of mRFP fluorescence and Iba1 signal revealed no co-localization between microglia and mRFP expressing astrocytes.

We also examined mRFP-p130PH expression in hippocampus after viral transduction. The same results as in the cortex were obtained, i.e., mRFP-p130PH was indeed expressed in astrocytes only, not in neuron and microglia. I also injected rAAV2/5 vectors with GFAP promoter and reporter gene mRFP into cortex and the same results were obtained, i.e., mRFP was selectively expressed in astrocytes.

3.6. Summary

Astrocytes are structurally and functionally interconnected with neurons and vasculature, thus, to understand their functions at the physiological and metabolic level are warranted. Our previous finding that astrocytes exhibit enhanced Ca^{2+} signaling in astrocytes following ischemia is very exciting and has offered a new perspective which drives us to further reveal the significant role of astrocytic Ca^{2+} signal in ischemic stroke. In our previous study we have demonstrated that cortical surface loading with BAPTA AM can selectively inhibit the ATP-induced Ca^{2+} signals in astrocytes, but not spontaneous neuronal Ca^{2+} signals. In the present study, we first buffered astrocytic Ca^{2+} signals using BAPTA AM, and the result shows that the infract volume caused by photothrombosis is significantly reduced, which raised the possibility that astrocytes contribute to neuronal death following ischemic injury.

Ca^{2+} increase in astrocytes also evoke other sequential events, such as glutamate release from astrocytes. To further test the hypothesis that Ca^{2+}-dependent glutamate release from astrocytes after ischemia contributes to neuronal damage, we tried a specific method — IP_3 binding protein p130PH — to inhibit astrocytic Ca^{2+}. The initial experiments conducted on both cultured primary astrocytes and cultured astrocytes cell lines show that mRFP-p130PH expressed in astrocytes can significantly inhibit ATP-induced Ca^{2+} signal. Expression of reporter protein mRFP does not affect the Ca^{2+} signal in astrocytes and therefore can be used as an expression marker to identify the p130PH expressing cells. Thus, inhibition of the IP_3 pathway using IP_3 binding protein p130PH can reduce Ca^{2+} signal dramatically in cultured astrocytes.

After proving the utility of p130PH in inhibiting Ca^{2+} in cultured astrocytes *in vitro*, we moved on to the *in vivo* level using living mouse to exam the functional role of p130PH protein in inhibiting astrocytic Ca^{2+} in mouse brain, and to test if inhibition of astrocytic Ca^{2+} will ameliorate neuronal damage through the reduction of glutamate release from astrocytes. To this end, for efficient and selective expression of our target gene mFP-p130PH in mouse brain, we have successfully constructed rAAV viral plasmids pZac2.1-ABC1D-mRFP-p130PH for positive experiments and pZac2.1-ABC1D-mRFP for control experiments. Astrocyte specific GFAP promoter ABC1D is introduced to direct transgene expression in astrocytes. Two weeks after microinjection with viral vectors pZac2.1-ABC1D-mRFP-p130PH into the cortex of mouse brain, transgene mRFP-p130PH was expressed in the cortex. GFAP staining demonstrates the high efficiency of viral transduction for astrocyte-specific expression of transgene driven by ABC1D promoter. Neither NeuN nor Iba1 signal was colocalized with mRFP fluorescence, proving that transgene mRFP-p130PH was indeed expressed in astrocytes only, not in neuron and microglia. Results of mRFP-p130PH expression in hippocampus after viral transduction were the same as those in the cortex, i.e., mRFP-p130PH was exclusively expressed in astrocytes. rAAV2/5 viral vectors with GFAP promoter and reporter gene mRFP was also injected into the cortex and the same results were obtained that mRFP was selectively expressed in astrocytes. These studies provide a solid foundation for the subsequent studies on the role of astrocyte Ca^{2+} signaling in neuronal death and brain damage in photothrombosis-induced ischemia in mice.

In conclusion, our work provides novel evidence that astrocytes contribute to brain injury after ischemia, and the inhibition of astrocytic Ca^{2+} might be the promising target

of stroke therapy. The current study will also provide an *in vivo* approach for the treatment of glia-related diseases as well as for the study on neuron-glia interactions in general.

3.7. Future work

Our further study will be focusing on determining whether p130PH will have a protective role on brain damage and neuronal death after a photothrombosis induced cerebral ischemic stroke. Using the photothrombosis ischemia model combined together with two-photon microscopy, we could provide a useful tool that can monitor cellular structure and physiological changes of astrocytes *in vivo* before and after induction of ischemia. The following two steps will be finished in the near future: 1) Ca^{2+} imaging in living mice with p130PH expressed in brain astrocytes will be done to see if inhibition of IP_3 pathway can also reduce *in vivo* astrocytic Ca^{2+}. 2) We would like to test if reduction of *in vivo* astrocytic Ca^{2+} signaling will have a protective effect in reducing neuronal damage after photothrombosis-induced ischemic stroke.

ABBREVIATIONS

Amp	Ampicillin
AMPA	α-amino-3-hydroxyl-5-methyl-4-isoxazole-propionate
AM	Acetoxymethyl
ATP	Adenosine-5'-triphosphate
BAPTA	1,2-bis(o-aminophenoxy)ethane-N,N,N',N'-tetraacetic acid
bp	Base pair
BSA	Bovinc serum albumin
CNS	Central nervous system
DAG	Diacylglycerol
dd H_2O	Double-distilled water
DI	Deionized
DMEM	Dulbecco's modified eagle medium
DMSO	Dimethyl sulfoxide
DPBS	Dulbecco's phosphate buffered saline
E. Coli	*Escherichia coli*
EDTA	Ethylenediaminetetraacetic acid
ER	Endoplasmic reticulum
FBS	Fetal bovine serum
GABA	γ-Aminobutyric acid
GFAP	Glial fibrillary acidic protein
GPCRs	G-protein coupled receptors
Iba1	Ionized calcium binding adaptor molecule 1
IP_3	Inositol 1, 4, 5-trisphosphate
IP_3BP	IP_3-binding proteins
IP_3R	Inositol triphosphate receptor
ITR	Inverted terminal repeat
kb	Kilobase

kDa	Kilodlton
LB	Luria-Bertani
MCS	Multiple cloning sites
NAD^+	Nicotinamide adenine dinucleotide
NeuN	Neuronal nuclei
NMDA	N-methyl-D-aspartic acid
PCR	Polymerase chain reaction
PFA	Paraformaldehyde
PH domain	Pleckstrin homology domain
PIP_2	Phosphatidylinositol 4, 5-bisphosphate
PLC	Phospholipase C
RNase	Ribonuclease
rAAV	Recombinant adeno-associated virus
RB	Rose bengal
rpm	Revotution per mintute
SAP	Shrimp alkaline phosphatase
SOB	Super optimal broth
SOC	SOB with added glucose
SR101	Sulforhodamine 101

REFERENCES

Agulhon C, Petravicz J, McMullen AB, Sweger EJ, Minton SK, Taves SR, Casper KB, Fiacco TA, McCarthy KD. 2008. What Is the Role of Astrocyte Calcium in Neurophysiology? Neuron. 59: 932-46.

Araque A, Li N, Doyle RT, Haydon PG. 2000. SNARE proteindependent glutamate release from astrocytes. J Neurosci. 20: 666–73.

Baltimore D, Mayer BJ, Ren R, Clark KL. 1993. A putative modular domain present in diverse signaling proteins. Cell. 73: 629–30.

Bezzi P, Gundersen V, Galbete JL, Seifert G, Steinha user C, Pilati E, Volterra A. 2004. Astrocytes contain a vesicular compartment that is competent for regulated exocytosis of glutamate. Nat Neurosci. 7: 613–20.

Brodal P. 1998. The Central Nervous System Structure and Function. 2nd ed. Oxford University Press. Chps 1, 2, 4. 1-53p. 148-176p.

Cearley CN, Wolfe JH. 2006. Transduction Characteristics of Adeno-associated Virus Vectors Expressing Cap Serotypes 7, 8, 9, and Rh10 in the Mouse Brain. Molecular Therapy. 13: 528-37.

Charles AC, Merrill JE, Dirksen ER, Sanderson MJ. 1991. Intercellular signaling in glial cells: calcium waves and oscillations in response to mechanical stimulation and goutamate. Neuron. 6: 983-92.

Cornell-Bell AH, Finkbeiner SM, Cooper MS Smith SJ. 1990. Glutamate induces calcium waves in cultured astrocytes: longrange glial singnaling. Science. 247: 470-3.

Davidson BL, Breakefield XO. 2003. Viral vectors for gene delivery to the nervous system. Nature Reviews Neuroscience. 4: 353-64.

Davidson BL, Stein CS, Heth JA, Martins L, Kotin RM, Derksen TA, Zabner J, Ghodsi A, Chiorini JA. 2000. Recombinant adeno-associated virus type 2, 4, and 5 vectors: Transduction of variant cell types and regions in the mammalian central nervous system. Proc Nat Acad Sci of the United States of America. 97: 3428-32.

Ding S, Wang T, Cui W, Haydon PG. 2009. Photothrombosis ischemia stimulates a sustained astrocytic Ca^{2+} signaling *in vivo*. Glia. In press.

Ding S, Fellin T, Zhu Y, Lee SY, Auberson YP, Meaney DF, Coulter DA, Carmignoto G, Haydon PG. 2007. Enhanced Astrocytic Ca^{2+} Signals Contribute to Neuronal Excitotoxicity after Status Epilepticus. J Neuroscience. 27: 10674 –84.

Dirnagl U, Iadecola C. Moskowitz MA. 1999. Pathobiology of ischaemic stoke: an integrated view. TINS. 22: 391-97.

Ferris CD, Snyder SH. 1992. IP_3 receptors. Ligand-activated calcium channels in multiple forms. Adv Second Messenger Phosphoprotein Res. 26: 95-107.

Fiacco TA, Agulhon C McCarthy KD. 2009. Sorting out Astrocyte Physiology from Pharmacology. Annu. Rev. Pharmacol. Toxicol. 49: 151-74.

Fisher KJ, Jooss K, Alston J, Yang Y, Haecker SE, High K, Pathak R, Raper SE, Wilson JM. 1997. Recombinant adeno-associated virus for muscle directed gene therapy. Nature Medicine. 3: 306-12.

Foskett JK, White C, Cheung KH, Mak DO. 2007. Inositol trisphosphate receptor Ca^{2+} release channels. Physiol Rev. 87: 593-658.

Haydon PG. 2001. Glia: Listening and talking to the synapse. Nature Reviews Neuroscience. 2: 185-93.

Haydon PG, Carmignoto G. 2006. Astrocyte Control of Synaptic Transmission and Neurovascular Coupling. Physiological Reviews. 86: 1009-101.

Hemmings BA, Haslam RJ, Koide HB. 1993. Pleckstrin domain homology. Nature. 363: 309–10.

Hill M. Cell Biology Course. The University of New South Wales, Sydney, Australia. http://cellbiology.med.unsw.edu.au/units/science/lecture0805.htm. Access date: Apr. 22, 2009

Kimelberg HK, Goderie SK, Higman S, Pang S, Waniewski RA. 1990. Swelling-induced release of glutamate, aspartate, and taurine from astrocyte cultures. The Journal of Neuroscience. 10: 1583-91.

Lee Y, Messing A, Su M, Brenner M. 2008. GFAP promoter elements required for region-specific and astrocyte-specific expression. Glia. 56: 481-93.

Lin X, Várnai P, Csordá G, Balla A, Nagai T, Miyawaki A, Balla T, Hajnóczky G. 2005. Control of Calcium Signal Propagation to the Mitochondria by Inositol 1, 4, 5-Trisphosphate-binding Proteins. The journal of Biological Chemistry. 280: 12820-32.

Manev H, Favaron M, Guidotti A, Costa E. 1989. Delayed increase of Ca^{2+} influx elicited by glutamate: role in neuronal death. Molecular Pharmacology. 36: 106-12.

Maton A, Hopkins J, McLaughlin CW, Johnson S, Warner M.Q, LaHart D., Wright JD. 1993. Human Biology and Health. Englewood Cliffs: Prentice Hall. 132–144p.

McCarthy KD, de Vellis J. 1980 Preparation of separate astroglial and oligodendroglial cell cultures from rat cerebral tissue. J Cell Biol. 85: 890-902.

Medical-dictionary: http://medical-dictionary.thefreedictionary.com/. Access date: Apr. 22, 2009

Nieuwenhuys R, Voogd J, Van Huijzen C. 2007. The Human Central Nervous System. 4th ed. Springer. 95-165p.

Nimmerjahn A, Kirchhoff F, Kerr JN, Helmchen F. 2004. Sulforhodamine 101 as a specific marker of astroglia in the neocortex *in vivo*. Nature Methods. 1: 31-37.

Riddihough G. 1994. More meanders and sandwiches. Nat. Struct. Biol. 1: 755–57.

SEER's training website: http://training.seer.cancer.gov/anatomy/nervous/tissue.html. Access date: Apr. 22, 2009

Sul JY, Orosz G, Givens RS, Haydon PG. 2004. Astrocytic connectivity in the hippocampus. Neuron Glia Biol. 1: 3-11.

Takano T, Tian GF, Peng W, Lou N, Libionka W, Han X, Nedergaard M. 2006. Astrocyte-mediated control of cerebral blood flow. Nat Neurosci 9:260–267.

Tenenbaum L, Chtarto A, Lehtonen E, Velu T, Brotchi J, Levivier M. 2004. Recombinant AAV-mediated gene delivery to the central nervous system. J Gene Med. 6: S212 - 22.

Várnai P, Lin X, Lee SB, Tuymetova G, Bondeva T, Spät A, Rhee SG, Hajnóczky G, Balla T. 2002. Inositol lipid binding and membrane localization of isolated pleckstrin homology (PH) domains. Studies on the PH domains of phospholipase C delta 1 and p130. J Biol Chem. 277:27412-22.

Wang X, Lou N, Xu Q, Tian GF, Peng WG, Han X, Kang J, Takano T, Nedergaard M. 2006. Astrocytic Ca^{2+} signaling evoked by sensory stimulation *in vivo*. Nat Neurosci 9: 816–23.

Wikipedia: http://en.wikipedia.org/wiki/Inositol_triphosphate. Access date: Apr. 22, 2009

Wilhelmsson U, Bushong EA, Price DL, Smarr BL, Phung V, Terada M, Ellisman MH, Pekny M. 2006. Redefining the concept of reactive astrocytes as cells that remain within their unique domains upon reaction to injury. Proceedings of the National Academy of Sciences of the United States of America. 103: 17513-18.

VITA

Wenju Cui was born in 1984 in Dalian, a beautiful coastal city in Liaoning Province, China. She was raised and went through grade schools in the same city. She graduated from Dalian Number Eight high school.

In July, 2007, after she obtained her bachelor's degree in Dalian University of Technology, majoring in Bioengineering, she was accepted by the Department of Biological Engineering at the University of Missouri in Columbia, Missouri, USA with an assistantship. After two years' study, in May, 2009, she received her master's degree.